WPS7826

Policy Research Working Paper 7826

Minimizing Ecological Damage from Road Improvement in Tropical Forests

Susmita Dasgupta
David Wheeler

WORLD BANK GROUP
Development Research Group
Environment and Energy Team
September 2016

Abstract

A spatial econometric model is used to link road upgrading to forest clearing and biodiversity loss in the moist tropical forests of Bolivia, Cameroon, and Myanmar. Using 250-meter cells, the model estimates the relationship between the rate of forest clearing in a cell and its distance to the urban market, with explicit attention given to road quality and simultaneity, terrain elevation and slope, the agricultural opportunity value of the land, and its legal protection status. Forest clearing is found to be most responsive to the distance to the nearest urban market, especially with secondary roads with lower typical speeds. Using the estimated forest-clearing response elasticities and a composite biodiversity indicator, an index of expected biodiversity loss from upgrading secondary roads to primary status is computed in each cell. The results identify areas in the three countries where high expected biodiversity losses may warrant additional protection as road upgrading continues. In addition, the results provide ecological risk ratings for individual road corridors that can inform environmentally sensitive infrastructure investment programs.

This paper is a product of the Environment and Energy Team, Development Research Group. It is part of a larger effort by the World Bank to provide open access to its research and make a contribution to development policy discussions around the world. Policy Research Working Papers are also posted on the Web at http://econ.worldbank.org. The authors may be contacted at sdasgupta@worldbank.org.

Minimizing Ecological Damage from Road Improvement in Tropical Forests

Susmita Dasgupta*
David Wheeler

This research was funded by the Knowledge for Change Program.

* Authors' names in alphabetical order. The authors are respectively Lead Environmental Economist, Development Research Group, World Bank and Senior Fellow, World Resources Institute.

Our sincere thanks to Siobhan Murray for GIS support. We are also thankful to Carter Brandon and Michael Toman for their very useful comments and suggestions.

1. Introduction

Protected-area strategies seek to conserve biodiversity in moist tropical forests by restricting infrastructure development in legally-demarcated zones. However, conflicts can arise when forested areas have significant agricultural potential. Within conservation areas, regulatory enforcement may be weakened by dominant economic interests. And some areas with high biodiversity value may be left unprotected so that development can proceed. By implication, both development and conservation may be hindered by a dichotomous policy regime that treats large areas as either completely protected or completely open for development. In reality, valuable economic and ecological resources have non-uniform, overlapping spatial distributions. Policy makers should therefore be equipped to weigh context-specific trade-offs between development and conservation objectives. This paper seeks to contribute by focusing on the trade-offs associated with road improvement in tropical forests. For three illustrative country cases in Latin America (Bolivia), Asia (Myanmar) and Africa (Cameroon), we develop and apply a high-resolution spatial model of road improvement impacts that includes both ecological risks and the economics of forest clearing. Our empirical work makes exclusive use of globally-available databases to ensure its applicability to all moist tropical forest countries.

The remainder of the paper is organized as follows. Section 2 reviews prior empirical research on the economics of forest clearing. In Section 3, we motivate our exercise with a theoretical economic model of road improvement and deforestation. Section 4 describes our spatially-formatted database, while Section 5 specifies and estimates a deforestation model that incorporates the impact of road improvement. In Section 6, we explore the implications of the results for our three cases. Section 7 develops an empirical framework for estimating the ecological impacts of road improvement, while Section 8 applies the framework to an assessment

of local and regional impacts in Bolivia, Cameroon and Myanmar. Section 9 summarizes and concludes the paper.

2. Prior Research

Empirical research has provided many useful insights about the determinants of forest clearing. The results are generally consistent with an economic model in which the conversion of forested land varies with potential profitability. Nelson and Chomitz (2009) and Rudel et al. (2009) have studied this relationship across countries over multi-year intervals. Within countries, numerous econometric studies have estimated the impact of economic, social and geographic drivers on deforestation during multi-year intervals. Some studies have used aggregate data for states, provinces or sub-provinces (e.g., studies for Brazilian municipios by Pfaff (1997) and Igliori (2006), and Mexican states by Barbier and Burgess (1996)).

Many studies have also used GIS-based techniques to obtain multi-year estimates at a higher level of spatial disaggregation (e.g., Cropper, et. al. (1999, 2001) for Thailand; Agwaral et al. (2002) for Madagascar; Deininger and Minton (1999, 2002), Chowdhury (2006) and Vance and Geoghegan (2002) for Mexico; Kaimowitz et al. (2002) for Bolivia; and De Pinto and Nelson (2009) for Panama). In rarer cases, studies have used annual national or regional aggregate time series for extended periods (e.g. Zikri (2009) for Indonesia; Ewers et al. (2008) for Brazil).

While econometric work on long-run deforestation drivers is well-advanced, previous data problems limited treatments of economic dynamics to theoretical work and simulation. Arcanda et al. (2008) and others studied the theoretical relationships between macroeconomic drivers and forest clearing. Notable simulation exercises include Cattaneo (2001) for Brazil and San et al. (2000) for Indonesia.

Recently, the advent of monthly and annual remote sensing databases has led to the first spatial estimation exercises that explicitly incorporate economic dynamics (Wheeler et al., 2011; Dasgupta et al., 2014). Direct impact studies in Latin America using the new databases have included high-resolution work on new road construction and deforestation in Brazil, where satellite monitoring has been available for a longer period (Laurance et al., 2009) and Bolivia, Panama, Paraguay and Peru (Reymondin et al., 2013).

More recently, Li et al. (2015) have investigated the potential impact of decreased travel time from improvement of road links in the Democratic Republic of Congo, but their cross-sectional analysis employs land use information (JRC 2003) that predates the new high-resolution satellite data. Damania and Wheeler (2015) have advanced the state of the art by estimating the potential impact of road upgrading on forest clearing and biodiversity in eight Congo Basin countries. Their deforestation model incorporates the latest high-resolution satellite data on forest cover changes, as well as quality estimates for specific links in the regional road system. They also create a biodiversity threat index that combines and synthesizes several measures of potential biodiversity loss.

This paper builds on the approach of Damania and Wheeler, while extending it in several ways. First, we broaden the research domain to include Latin America and Asia. Second, we gain precision by operating at higher spatial resolution. Third, we generalize the methodology by substituting globally-available road quality estimates for the Africa-specific estimates employed in the previous work. Finally, we expand the previously-developed biodiversity indices for the Congo Basin countries into a global database that includes a larger set of biodiversity measures.

3. Modeling the Economics of Road Improvement and Deforestation

From a formal analytical perspective, this research treats road improvement as a problem of competitive selection among corridors that traverse the same region. The corridors differ in length, construction cost conditions, biodiversity value and potential agricultural income. The optimum corridor choice reflects maximization of a social utility function that values both income and biodiversity, subject to a fixed budget constraint, feasible road quality improvement in each corridor (reflecting the budget constraint), and the corridor-specific impacts of road quality improvement on potential biodiversity loss, expected income growth in the corridor, and expected income growth from increased trade between areas connected by the corridor.

We motivate the following econometric analysis with a model that specifies the basic determinants of road improvement impacts and explores their economic and ecological dimensions.[1] For expositional clarity and simplicity, we use the Cobb-Douglas (constant-elasticity) specification for all profit and cost functions. This specification is linear in the logs of equation variables and is a first-order approximation to more general specifications (CES, translog, etc.). To simplify the theoretical analysis of alternatives, we assume a constant road improvement budget. Applied assessments of road improvement alternatives might also consider cases where road quality is held constant and improvement expenditures differ because corridors differ in length. In such cases, estimated improvement costs would be subtracted from estimated income gains to provide the appropriate comparison.

[1] The theoretical model in this section was first developed by one of the co-authors (Wheeler) in collaborative work with Richard Damania on road upgrading and forest clearing in the Congo Basin countries (Damania and Wheeler, 2015). Many thanks to Richard for his insights and suggestions.

3.1 Interregional Trade

We specify the economic value of trade between areas connected by a road corridor with a standard gravity model, augmented by a measure of road quality. For a prior application of this approach to overland trade expansion, see Buys, Deichmann and Wheeler (2010).

(1) $T_{ij} = \propto_0 E_i^{\propto_1} E_j^{\propto_2} d_{ij}^{-\propto_3} q_{ij}^{\propto_4}$

where $\alpha_0, \alpha_1, \alpha_2, \alpha_3, \alpha_4 > 0$

T_{ij}	=	Value of trade between areas i and j
E_i, E_j	=	Economic scale of areas i and j
d_{ij}	=	Road distance between areas i and j
q_{ij}	=	Quality of the road linking areas i and j ($0 \leq q \leq 1$, where 0 → forest track and 1 → paved 1st class road)

An improvement in road quality (q) lowers transport costs and increases the potential profitability of agricultural production in the road corridor. The budget for maintaining a particular road quality level is given by:

(2) $B = \gamma_0 q^{\gamma_1} d \quad (\gamma_1 > 1)$

For a fixed road quality budget B:

(3) $q = [\frac{B}{\gamma_0}]^{\frac{1}{\gamma_1}} d^{-\frac{1}{\gamma_1}}$

In (3), given a fixed road quality budget, road quality declines with road length. The rate of decline depends on the cost elasticity of road quality. Substituting (3) into (1) and simplifying, an increase in the road improvement budget ($B_1 \rightarrow B_2$) has the following impact on trade between areas i and j:

(4) $\frac{T_{ij2}}{T_{ij1}} = [\frac{B_2}{B_1}]^{\frac{\propto_4}{\gamma_1}}$

The interpretation of (4) is straightforward: Trade between areas i and j will expand more or less proportionately with the road improvement budget, depending upon whether the road quality elasticity of trade is greater than or less than the cost elasticity of road quality.

3.2 Local Profitability and Forest Clearing

An improvement in road quality lowers transport costs and increases the expected profitability of agricultural production in a road corridor. The expected profitability of agricultural production increases with the size of a cleared parcel, which is determined by the distance of the forest clearing limit from the road. With both factors taken into account, the expected profit function for each unit of road frontage is:[2]

(5) $\pi = \beta_0 v^{\beta_1} q_{ij}^{\beta_2} h^{\beta_3}$

where $\beta_0, \beta_1, \beta_2 > 0, 0 < \beta_3 \leq 1$
π = Potential profit from land clearing
v = Potential agricultural value per hectare
h = Distance of forest-clearing limit from the road

The proprietor of each road-front parcel also confronts incremental forest clearing costs that are constant or increasing with distance from the road and, for agricultural production, incremental commodity transport costs that increase with distance from the road. The proprietor's composite cost function is:

(6) $C = \delta_0 h^{\delta_1}$ ($\delta_1 > 1$)

With (5) and (6) specified as present values, the optimal clearing distance from the road is determined by the equality of marginal expected profits and clearing costs. Taking appropriate derivatives, substituting and simplifying, the optimal clearing distance is given by:

(7) $h^* = \theta B^{(\frac{\mu}{\delta_1-\beta_3})} v^{(\frac{\beta_1}{\delta_1-\beta_3})} d^{-(\frac{\mu}{\delta_1-\beta_3})}$

where $= \beta_2/\gamma_1$, $\delta_1 - \beta_3 > 0$ (from (5) and (6)) and θ is a composite of equation constants.

[2] We incorporate potential profits without explicit assumptions about local price dynamics. Local profitability (and forest-clearing responses) will be greater if farmers are price-takers in regional markets. The clearing response to road investment will be smaller in cases where production from newly-cleared land is sufficient to reduce farm gate prices. We are indebted to our colleague Carter Brandon for this point.

In (7), the composite elasticities of B, v and d are positive, positive and negative, respectively. Responsiveness increases in each case as the difference narrows between the cost and profit elasticities of forest clearing (δ_1 and β_3). The responsiveness of forest clearing to greater spending on road quality and greater road distance increases with the ratio of the profit and cost elasticities of road quality.

Appropriate substitution and simplification yield the following expression for total profit in the road corridor:

(8) $\Pi = 2d\pi(h^*) = PB^{\rho\mu}v^{\rho\beta_1}d^{1-\rho\mu}$

where P is a composite of equation constants and $\rho = \frac{1+\beta_3}{\delta_1-\beta_3}$ (> 1).

In (8), total expected profits rise less than proportionally with road distance, since expected profits for each roadside land parcel fall as road distance increases. The sign of the distance elasticity in (8) is ambiguous, since $\rho\mu$ can be greater or less than one. In the former case, total profits will actually fall as road distance increases. From (8), an increase in the road improvement budget ($B_1 \rightarrow B_2$) has the following impact on total profits in a road corridor:

(9) $\frac{\Pi_2}{\Pi_1} = [\frac{B_2}{B_1}]^{\rho\mu}$

In (9), total road corridor profits increase more or less proportionately with the road quality budget, depending upon whether $\rho\mu$ is greater or less than one. The overall interpretation of (9) is as follows: For a road corridor, the responsiveness of total profits to an increase in the road quality budget is positively related to the ratio of profit and cost elasticities of road quality, positively related to the profit elasticity of forest clearing, and negatively related to the difference between the cost and profit elasticities of forest clearing.

3.3 Biodiversity Loss

Substituting from (7), total biodiversity loss in a road corridor is given by:

$$(10)\ L = 2d\varepsilon h^* = 2\varepsilon\theta B^{(\frac{\mu}{\delta_1-\beta_3})} v^{(\frac{\beta_1}{\delta_1-\beta_3})} d^{1-(\frac{\mu}{\delta_1-\beta_3})}$$

where ε = Measured biodiversity intensity

In (10), the relationship between total biodiversity loss and road distance depends on whether the ratio of the profit and cost elasticities of road quality is greater than the difference between the cost and profit elasticities of forest clearing. If this is the case (given a fixed budget for road quality), total biodiversity loss will decline with road distance. If the converse is true, increasing road distance will increase biodiversity loss.

From (10), the relationship between a road budget increase and total biodiversity loss is given by:

$$(11)\ \frac{L_2}{L_1} = [\frac{B_2}{B_1}]^{(\frac{\mu}{\delta_1-\beta_3})}$$

As above, biodiversity loss will increase more than proportionately with a road budget increase if the ratio of profit and cost elasticities of road quality is greater than the difference between the cost and profit elasticities of forest clearing.

For a fixed road quality budget, the relative profit and biodiversity loss equations for two competitive road corridors (A and B) are as follows:

$$(12)\ \frac{\Pi_A}{\Pi_B} = \left[\frac{v_A}{v_B}\right]^{\rho\beta_1} \left[\frac{d_A}{d_B}\right]^{1-\rho\mu}$$

$$(13)\ \frac{L_A}{L_B} = \frac{\varepsilon_A}{\varepsilon_B} \left[\frac{v_A}{v_B}\right]^{(\frac{\beta_1}{\delta_1-\beta_3})} \left[\frac{d_A}{d_B}\right]^{1-(\frac{\mu}{\delta_1-\beta_3})}$$

Ceteris paribus (i.e., for identical road budgets and biodiversity intensities), the corridor with greater potential agricultural value per hectare will have both higher total profits and greater total biodiversity loss. The effects of road distance are more complex for two reasons. First:

$$(14)\ \rho\mu - \frac{\mu}{\delta_1-\beta_3} = \frac{1+\beta_3}{\delta_1-\beta_3}\mu - \frac{1}{\delta_1-\beta_3}\mu = \frac{\beta_3}{\delta_1-\beta_3}\mu\ (>0)$$

Given (14), equations (12) and (13) incorporate three possibilities. Let $\eta_1 = \rho\mu$ and $\eta_2 = \mu/(\delta_1-\beta_3)$. If η_1 and η_2 are both less than one, the corridor with the longer road will have greater total profits and greater biodiversity loss. If η_1 and η_2 are both greater than one, the corridor with the longer road will have lower profits and lower biodiversity loss. In the third possible case -- $\eta_1 > 1$ and $\eta_2 < 1$ -- the corridor with the *shorter* road will be favored unambiguously because it will have higher profits and lower biodiversity loss. It is important to note that this is a ceteris paribus result, since the corridor with the shorter road could have sufficiently greater biodiversity intensity to reverse the result. A complete calculation would also have to include consideration of trade-related regional income, which would favor the shorter road. Given the relatively complex set of factors that affect these results, the impacts of road improvement on income gains, forest clearing and biodiversity loss seem likely to vary significantly across countries, and across regions within countries. In this paper, we focus on the forest clearing and biodiversity components of the problem.

4. Data

4.1 Road Networks

Table 1 and Figure 1 summarize 2014 road network information for Bolivia, Cameroon and Myanmar in digital maps (shapefiles) provided by Delorme, Inc. As Table 1 shows, the maps identify 4,607 road links in Bolivia, 2,951 in Cameroon and 6,980 in Myanmar. Network links are graded by status: secondary roads (orange in Figure 1), primary connector roads (red), and primary highways (purple).

Table 1: Road links by network status: Bolivia, Cameroon and Myanmar

Road Links	Bolivia	Cameroon	Myanmar
Secondary Roads	3,760	2,162	4,879
Primary Roads	847	789	2101

Total	4,607	2,951	6,980

Figure 1: Road networks: Bolivia, Cameroon and Myanmar

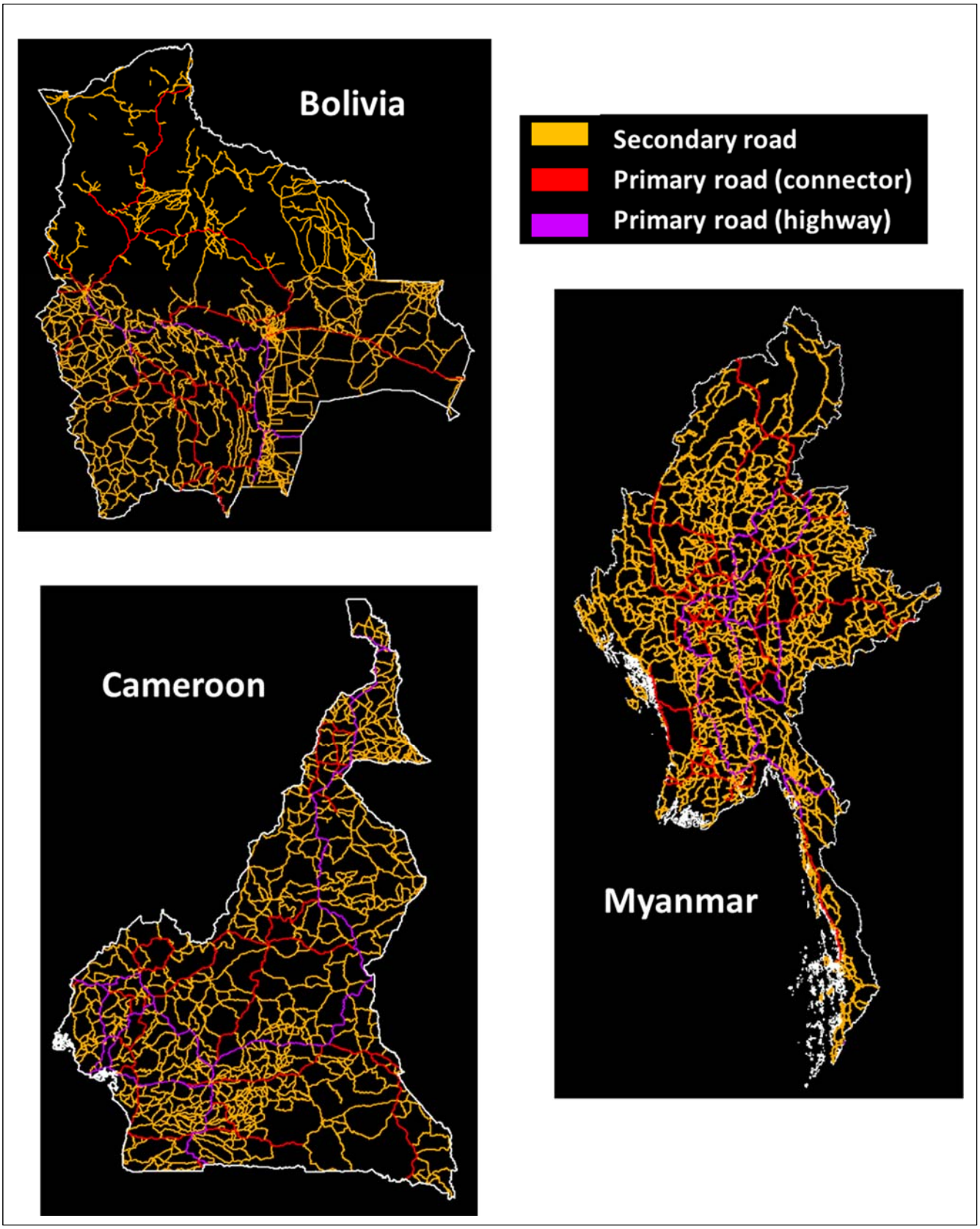

4.2 Forest Clearing

Hansen et al. (2013) publish annual high-resolution estimates of global forest clearing. The data are currently available at 30 m spatial resolution for 2000-2014. For this research, we have created annual files in which cleared pixels are assigned the value 1 in the year when most clearing occurred. Uncleared pixels are assigned the value 0. We focus on areas defined as moist tropical forest ecoregions by WWF (see Sections 5.2 and 7.3).[3] We use the Hansen estimates to compute forest clearing rates in 250 m cells.[4] Edge effects, non-forest areas and other factors cause Hansen pixel counts to vary somewhat by cell. We standardize by computing the annual cumulative percent cleared in each cell through 2014.[5]

Figure 2 displays our estimates for representative moist forest areas in Bolivia, Cameroon and Myanmar. Each cell is color-coded by cumulative percent cleared in 2001-2014. The figure reveals a striking pattern of deforestation along some of the roads in the Delorme database. Along other roads, however, deforestation is much less pronounced.

[3] For a complete list of WWF ecoregions, see http://wwf.panda.org/about_our_earth/ecoregions/ecoregion_list/.
[4] We use the 250 m approximation for expositional convenience. Our cell sides are .0025 decimal degrees in length. This translates to 278.3 meters on a side, yielding cell areas of 77,450.9 square meters or 7.75 hectares.
[5] Our estimate also incorporates the Hansen 30 m estimates of tree cover in 2000.

Figure 2: Forest clearing and road networks, 2000-2014

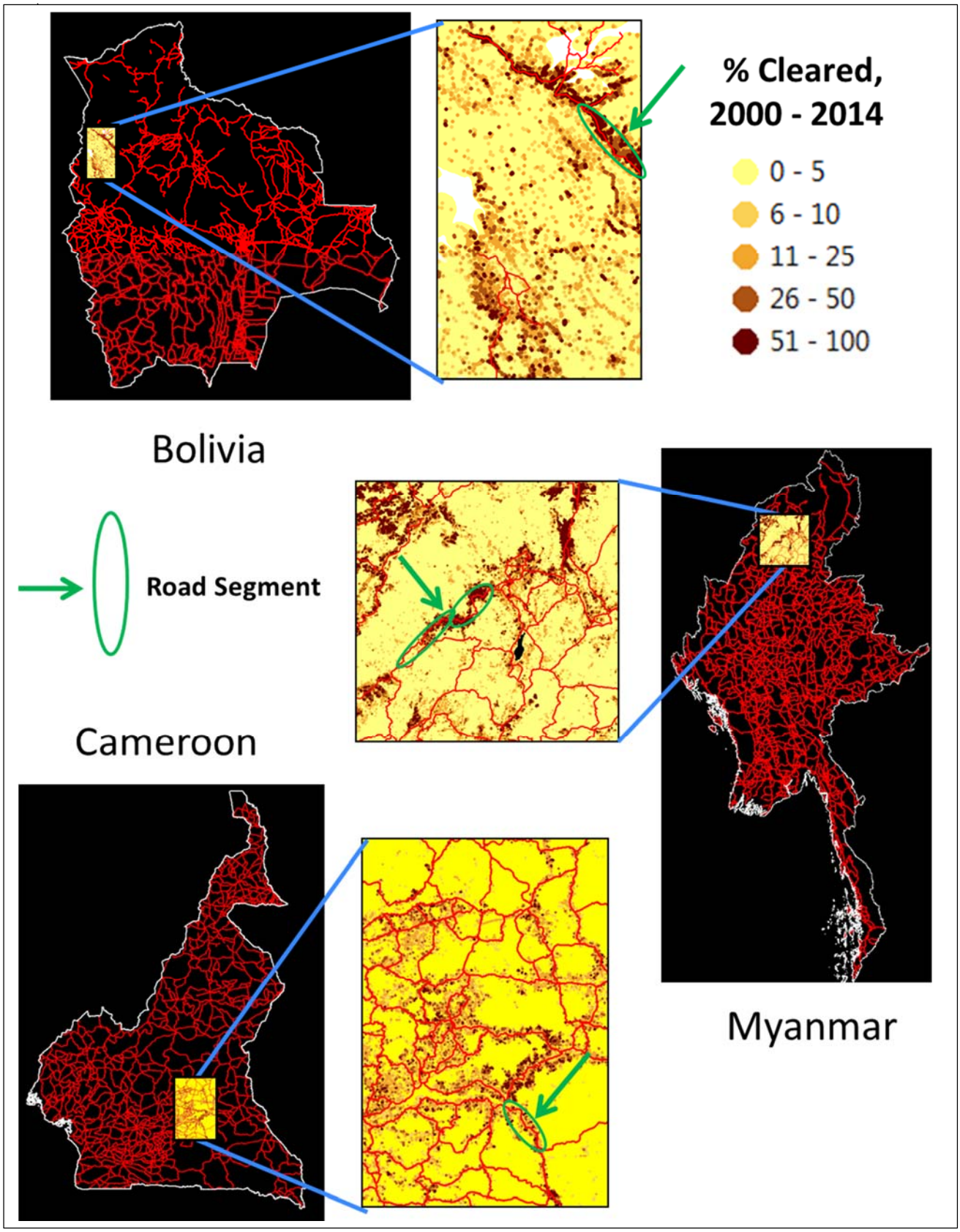

Figure 2 also identifies road segments that we use to illustrate the relationships between clearing activity and distance from the nearest road. For each country and segment, Figure 3 displays two overlapping graphs. The first is a scatter diagram of changes in percent cleared (2000-2014) vs. distance from the road segment, produced using 5,000 randomly-selected 250 m cells within 20 km of the road. To produce the second graph, we round to the nearest kilometer of distance for all cells within 20 km of the road; calculate the mean change in percent cleared (2000-2014) for each km; and draw connecting lines.

The mean line provides a clear interpretation of the information in the scatter diagrams. As distance from the road increases, all three graphs reveal a steep fall in mean percent cleared for the first 5 km, a declining slope through 10 km, and approximate flattening near zero beyond 10 km. Although the shapes of change/distance relationships are similar for the three countries, it is worth noting that the magnitudes are quite different. From 2000 to 2014, mean clearing within half a kilometer of the road increases by nearly 20 percentage points in Bolivia and 15 points in Myanmar, but only 5 points in Cameroon.

The basic shape of the clearing/distance relationship illustrated in Figure 3 can be captured by an exponential function that we employ for the econometric analyses in this paper:

(15) $p = \beta_0 h^{\beta_1}$

where $\beta_1 < 0$
p = Change in percent cleared in a 250 m cell
h = The cell's distance from the road

For econometric work, we translate the function to its linear form in the logarithms of h and p.

5. Estimation of the Forest Clearing Model

The estimation exercise in this paper draws on the insights of previous research and the theoretical model in Section 3 to incorporate five critical determinants of forest clearing in road

Figure 3: Change in percent cleared (2000-2014) vs. distance from road segments

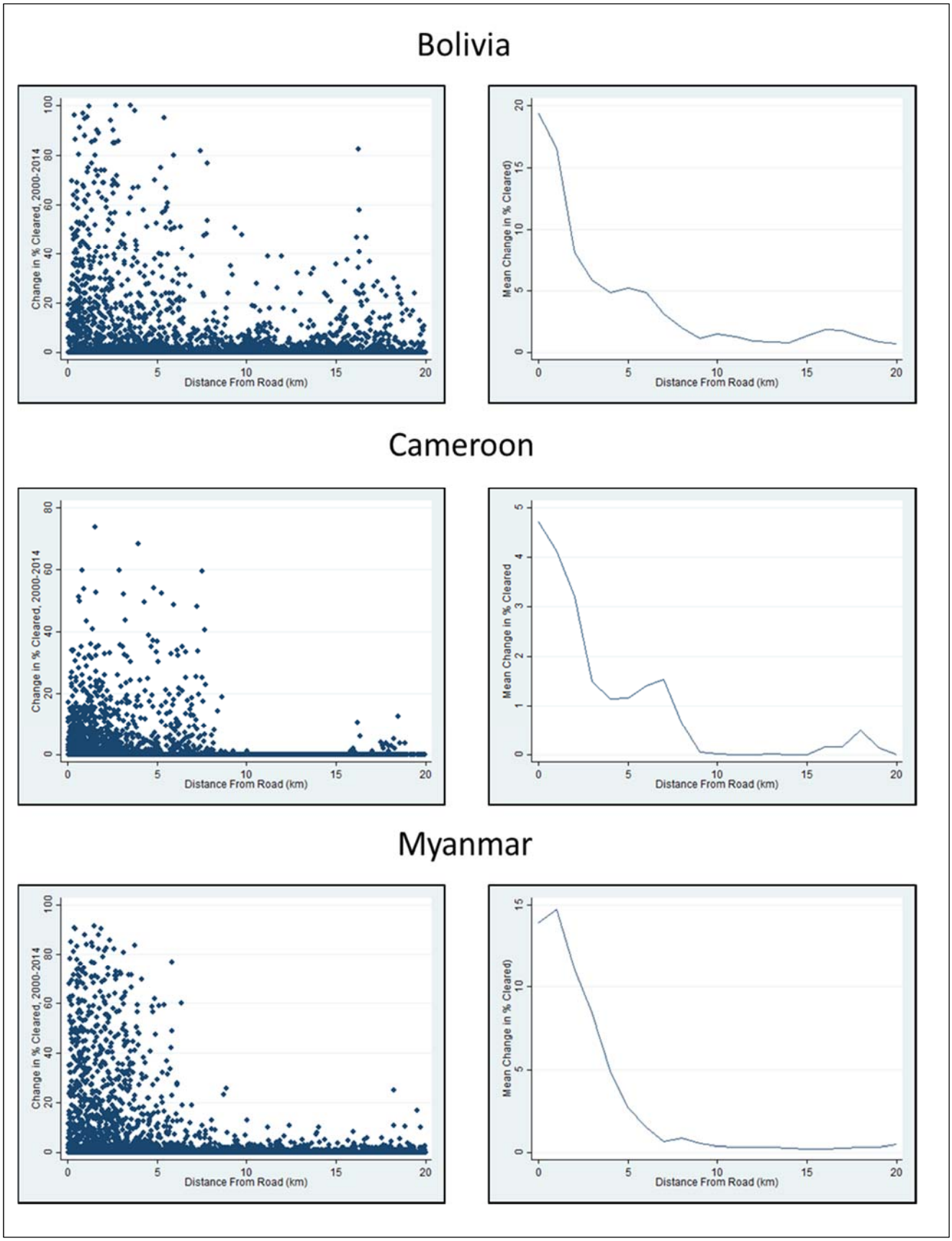

corridors: distance from the road, transport cost to the nearest market center, the agricultural opportunity value of the land, terrain slope, and legal protection status. We extend previous work on road transport cost and deforestation by introducing explicit estimation of road quality effects in a network access model. First, we divide all road segments into 500 m increments and use GIS to determine the network path with the shortest travel distance from each increment midpoint to an urban center with 50,000+ population. Then we separate the distance into the parts traveled on secondary and primary roads.

5.1 Model Specification

The dependent variable in our estimating equation (16) is a decimal percentage, so we impose the appropriate asymptotic limits [0,1] by specifying the forest clearing rate as a log-odds ratio.

(16) $f_i = \beta_0 + \beta_1 \ln d_{ij} + [\beta_2 + \beta_3 \gamma_{ij}] \ln D_{ij} + [\beta_4 + \beta_5 \ln e_i] \ln s_{ij} + \beta_6 \ln p_i + \beta_7 \ln a_i + \varepsilon_i$

Expected signs: $\beta_1, \beta_2, \beta_4, \beta_6 < 0$; $\beta_3, \beta_7 > 0$

where

$f_i = \ln\left[\frac{c_i}{1-c_i}\right]$

c_{ij} = Cumulative percent cleared in 2014, cell i
d_{ij} = Distance of cell i from nearest road segment j
D_{ij} = Shortest network distance from i via segment j to the nearest urban center
γ = Primary road share of distance from i to the nearest urban center
s_i = Slope of cell i (measured as within-cell standard deviation of elevation)
e_i = Elevation of cell i
p_i = Legal protection status of cell i
a_i = Agricultural opportunity value of land in cell i
ε_{it} = Random error term

A priori, we expect the impact on forest clearing to be negative for distance from the nearest road ($\beta_1 < 0$); negative for travel distance to the nearest urban center ($\beta_2 < 0$), moderated by the share of primary roads traveled ($\beta_3 > 0$); negative for more steeply-sloped terrain ($\beta_4 < 0$), possibly affected by average elevation ($\beta_5 \gtreqless 0$); negative for legal protection status ($\beta_6 < 0$),

although this will be affected by country-specific enforcement factors; and positive for the agricultural opportunity value of the land ($\beta_7>0$).

5.2 Estimation Areas

We estimate the model for all cells in WWF's moist tropical forest ecoregions of each country, which are discussed more fully in Section 7. Figures 4-6 identify the relevant ecoregions, which dominate northern and central Bolivia, southern Cameroon, and most of Myanmar.

5.3 Variable Measures

Our data and sources are as follows.

Hansen pixels cleared: per 250 m cell, the percent of 30 m Hansen pixels cleared. This incorporates two measures: percent cleared prior to 2001, and annual clearing from 2001 to 2014 (Hansen et al. (2013)).

Distance from road segment: distance from the centroid of each cell to the nearest road segment, calculated in ArcGIS 10.

Distance traveled to the nearest urban center via secondary and primary road segments: Calculated in ArcGIS 10 from Delorme digital road maps.

Elevation: Average elevation for a cell, calculated from the CGIAR-SRTM dataset (3 seconds resolution), aggregated to 30 seconds resolution by DIVA-GIS (http://www.diva-gis.org/gdata).

Terrain slope: Standard deviation of pixel-level elevation measures within a cell.

Legal protection status: 1 if the cell is in a protected area identified by the World Database on Protected Areas (WDPA); 0 otherwise. The WDPA shapefile has been downloaded from http://www.protectedplanet.net/.

Agricultural opportunity value: mean value for a cell, calculated from the high-resolution global grid developed by Deveny et al. (2009). Raster resolution: .0025 decimal degrees. The Deveny data have been drawn from two sources: (1) Foregone agricultural rents from Naidoo and Iwamura (2007), who integrate spatial information on crop productivity, livestock density, and prices to produce a global map of the gross economic rents from agricultural lands. (2) Spatially-explicit calculation by Kindermann et al. (2006) of income foregone from a one-time timber harvest when timber rents exceed agricultural rents.

Figure 4: Bolivia - Moist forest ecoregions

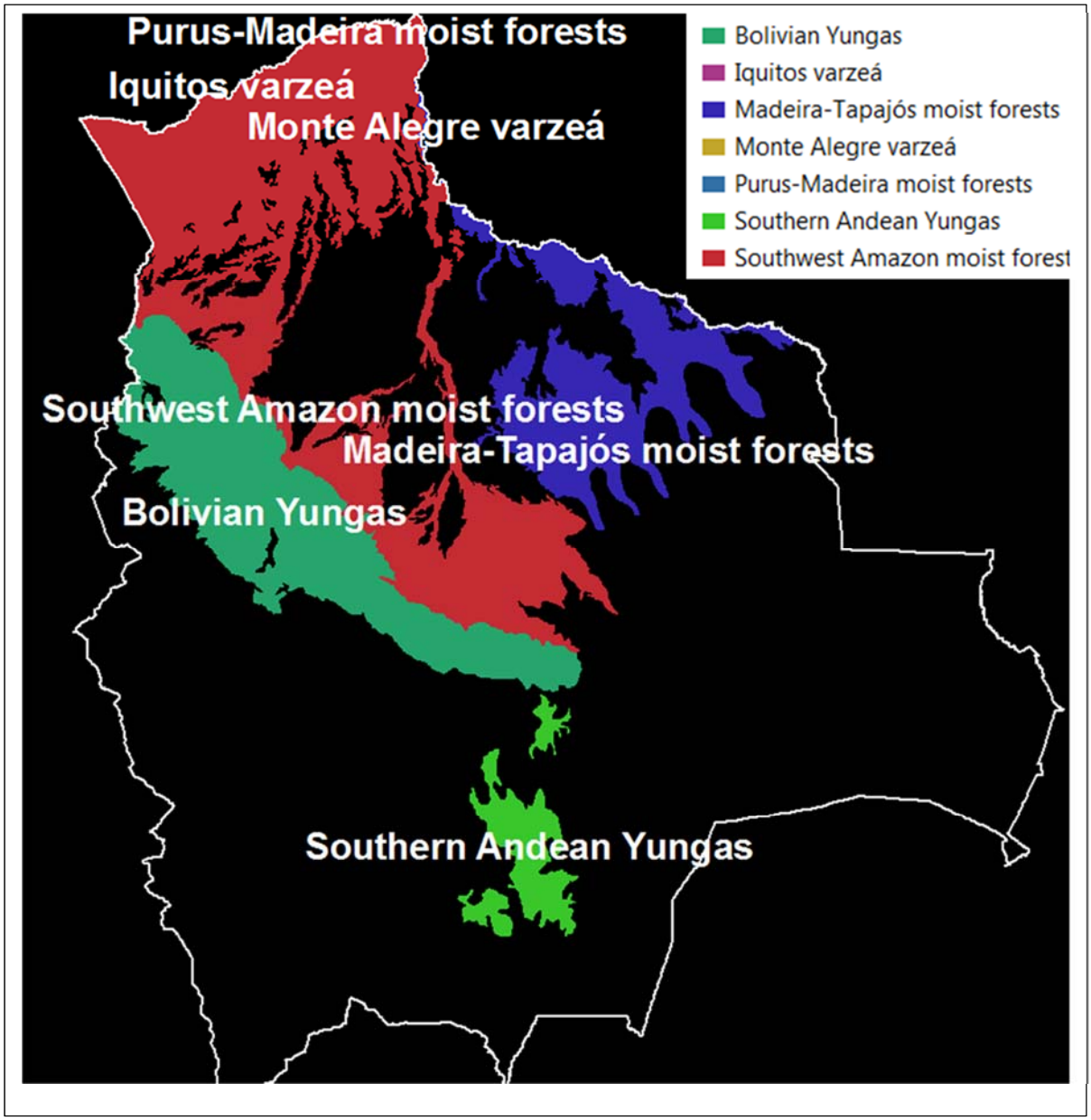

Figure 5: Cameroon - Moist forest ecoregions

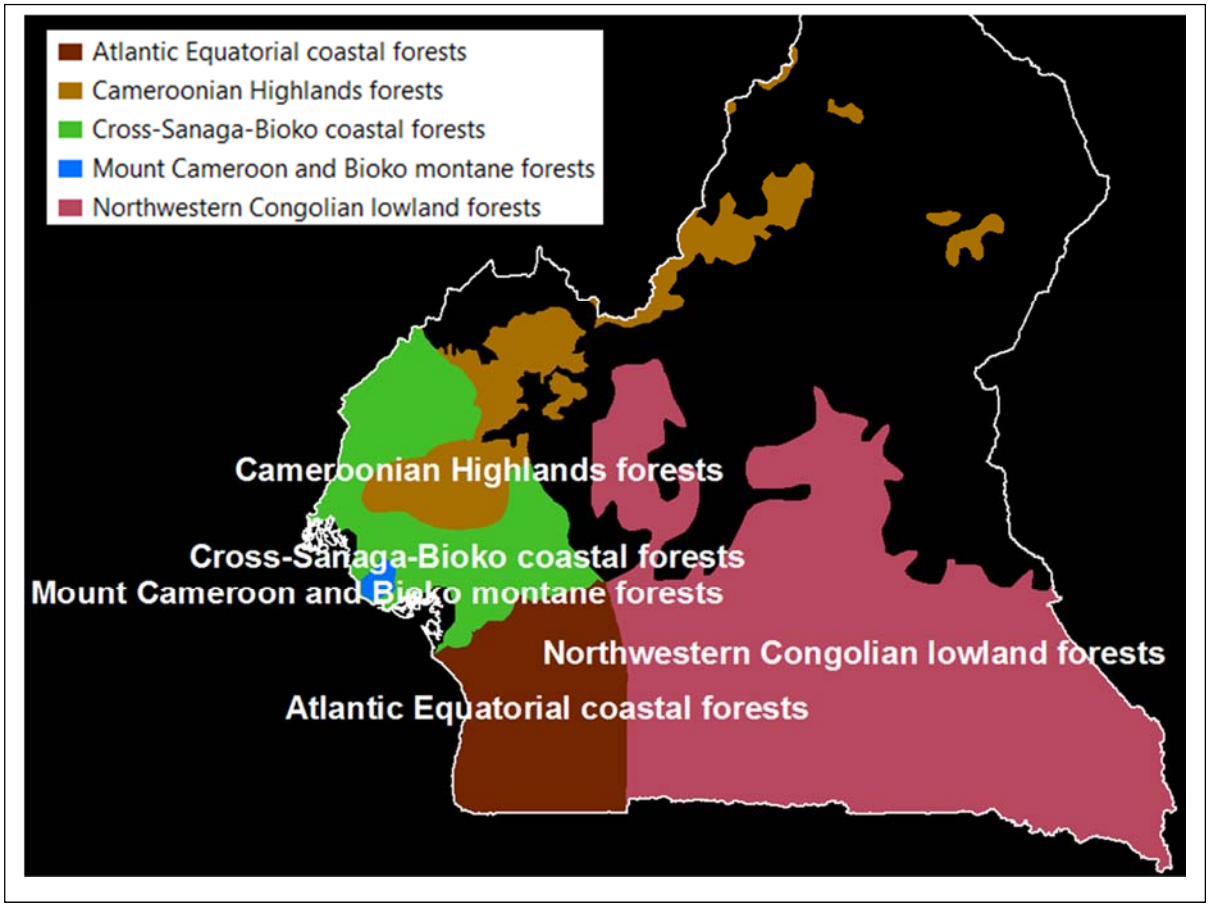

Figure 6: Myanmar - Moist forest ecoregions

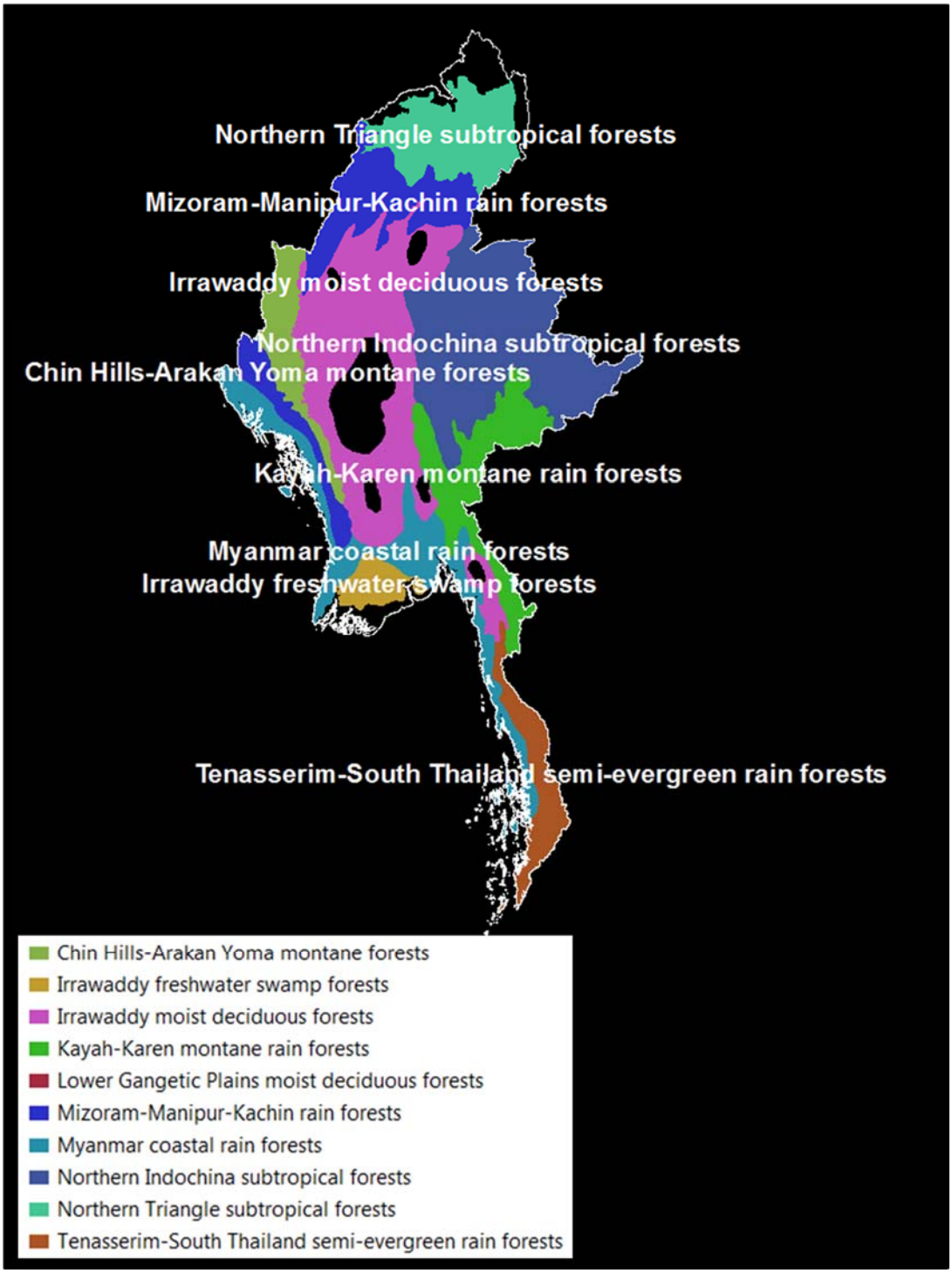

5.4 Estimation

In this exercise, we have addressed two potentially-significant estimation issues. The first is simultaneity between forest clearing and distance to the nearest urban center. As Damania and Wheeler (2015) and others have noted, road location may be related to the relative profitability of forest clearing. We address this problem via instrumental variables, using geodetic distance from each road increment midpoint to the nearest urban center as our instrument.

The second potential problem is spatial autocorrelation, which may have significant effects on our regression results. We address this problem with a spatial econometric estimator,[6] using the inverse-distance specification of the spatial weights matrix.

Tables 2-4 present our estimation results for three sample sizes. The first three columns in the tables present estimates for randomly-drawn samples of 10,000 cells. These are dispersed across enormous cell populations in very large areas in Bolivia (3.4 million cells), Cameroon (3.3 million), and Myanmar (5.8 million). A priori, we would expect this dispersal to minimize the estimation bias and inconsistency produced by spatial autocorrelation among neighboring cells.

Columns (1-3) present results for instrumental variables (IV) (1), IV with bootstrapped standard errors (a robustness check, calculated from more-dispersed subsamples of 5,000 observations) (2), and spatial econometric estimation using IV (3). We also include IV and bootstrapped IV estimates (from 20,000-observation subsamples) for much larger randomly-drawn samples (20% for each country), and for all cells in each country. We are unable to provide spatial econometric estimates for the 20% and full samples because calculation of spatial weights matrices is infeasible for such huge observation sets.

[6] We use the Stata estimator spreg.

In any case, the results in Tables 2-4 are reassuring: For each country, all estimated parameters have the expected signs and very high statistical significance. Within each country, the estimates are quite stable across sample sizes and estimation modes. To facilitate comparison, Table 5 presents median parameter estimates.

Table 5: Median parameter estimates

Variable	Bolivia	Cameroon	Myanmar
Distance from road	-0.326	-0.094	-0.181
Distance to nearest urban center (DU)	-0.530	-0.372	-0.336
DU x Primary road share	0.209	0.192	0.060
Slope (Std. dev. of elevation)	-0.812	-0.543	-0.467
Slope x Elevation	0.148	0.067	0.044
Protected area	-0.236	-0.327	-0.780
Agricultural opportunity value	0.364	0.389	0.075
Constant	-1.357	-0.006	1.324

As previously noted, all parameter estimates for all three countries have the expected signs and significance levels greater than 99%. We highlight results for the distance-related variables.[7] The median elasticity of distance from the road is greatest for Bolivia (-0.326) and least for Cameroon (-0.094). The same pattern holds for distance to the nearest urban center and its interaction with the share of primary roads traveled. For Bolivia, the median elasticity is -0.530 for travel solely on secondary roads and -0.321 (-0.530 + 0.209) for travel solely on primary roads. Cameroon has lower elasticities for travel solely on secondary roads (-0.372) and primary roads (-0.18), while Myanmar is similar to Cameroon for secondary roads (-0.336) and Bolivia for primary roads (-.276).

[7] Given our model specification, each parameter estimate is interpreted as the elasticity of the log-odds ratio for forest clearing with respect to the relevant righthand variable.

Table 2: Regression Results: Bolivia

All variables in logs except the dummy variable for protected status

Dependent variable: Log odds ratio, cumulative forest cleared %, 2014

	Random Sample (10,000 obs.)			20% Random Sample		All Observations	
	OLS (1)	Bootstrap (2)	Spatial (3)	OLS (4)	Bootstrap (5)	OLS (6)	Bootstrap (7)
Distance from road	-0.326	-0.326	-0.323	-0.323	-0.323	-0.327	-0.327
	(15.39)**	(12.03)**	(15.34)**	(129.25)**	(21.37)**	(292.22)**	(25.03)**
Distance to nearest urban center (DU)	-0.499	-0.499	-0.488	-0.531	-0.531	-0.530	-0.530
	(11.79)**	(7.33)**	(11.67)**	(104.99)**	(15.56)**	(234.72)**	(16.77)**
DU x Primary road share	0.215	0.215	0.209	0.209	0.209	0.209	0.209
	(16.88)**	(11.78)**	(16.60)**	(137.29)**	(19.56)**	(307.60)**	(26.71)**
Slope (Std. dev. eleveation)	-0.797	-0.797	-0.772	-0.812	-0.812	-0.828	-0.828
	(7.79)**	(5.01)**	(7.59)**	(66.22)**	(11.48)**	(150.89)**	(12.65)**
Slope x Elevation	0.148	0.148	0.143	0.147	0.147	0.149	0.149
	(10.54)**	(7.04)**	(10.26)**	(87.73)**	(16.25)**	(198.87)**	(17.63)**
Protected area	-0.245	-0.245	-0.246	-0.236	-0.236	-0.236	-0.236
	(4.19)**	(3.11)**	(4.23)**	(33.70)**	(5.22)**	(75.20)**	(6.97)**
Agricultural opportunity value	0.356	0.356	0.354	0.367	0.367	0.364	0.364
	(14.84)**	(10.93)**	(14.84)**	(126.99)**	(20.63)**	(282.02)**	(24.57)**
Constant	-1.559	-1.559	-1.059	-1.357	-1.357	-1.341	-1.341
	(6.69)**	(4.13)**	(4.13)**	(48.30)**	(7.59)**	(106.77)**	(7.11)**
Observations	9,998	9,998	9,998	705,260	705,260	3,526,359	3,526,359
R-squared	0.20	0.20		0.19	0.19	0.19	0.19

Absolute value of t statistics in parentheses
* significant at 5%; ** significant at 1%

Table 3: Regression Results: Cameroon

All variables in logs except the dummy variable for protected status

Dependent variable: Log odds ratio, cumulative forest cleared %, 2014

	Random Sample (10,000 obs.)			20% Random Sample		All Observations	
	IV	Bootstrap IV	Spatial IV	IV	Bootstrap IV	IV	Bootstrap IV
	(1)	(2)	(3)	(4)	(5)	(6)	(7)
Distance from road	-0.097	-0.097	-0.094	-0.094	-0.094	-0.093	-0.093
	(11.21)**	(6.64)**	(11.06)**	(85.35)**	(13.74)**	(188.37)**	(13.83)**
Distance to nearest urban center (DU)	-0.374	-0.374	-0.345	-0.370	-0.370	-0.372	-0.372
	(27.54)**	(20.84)**	(25.39)**	(223.72)**	(30.90)**	(501.44)**	(42.74)**
DU x Primary road share	0.187	0.187	0.177	0.192	0.192	0.192	0.192
	(29.47)**	(18.53)**	(28.08)**	(237.17)**	(34.52)**	(530.80)**	(38.13)**
Slope (Std. dev. of elevation)	-0.499	-0.499	-0.515	-0.551	-0.551	-0.543	-0.543
	(12.19)**	(10.37)**	(12.78)**	(104.31)**	(20.61)**	(229.91)**	(17.86)**
Slope x Elevation	0.061	0.061	0.063	0.068	0.068	0.067	0.067
	(10.52)**	(8.20)**	(11.02)**	(90.44)**	(15.71)**	(199.75)**	(15.82)**
Protected area	-0.363	-0.363	-0.366	-0.325	-0.325	-0.327	-0.327
	(12.65)**	(8.72)**	(12.94)**	(89.78)**	(16.53)**	(201.42)**	(16.25)**
Agricultural opportunity value	0.388	0.388	0.375	0.391	0.391	0.389	0.389
	(43.30)**	(31.24)**	(42.08)**	(342.24)**	(67.15)**	(761.91)**	(58.52)**
Constant	0.003	0.003	0.192	-0.007	-0.007	-0.006	-0.006
	(0.04)	(0.03)	(2.74)**	(0.82)	(0.12)	(1.55)	(0.13)
Observations	10,000	10,000	10,000	645,901	645,901	3,229,507	3,229,507
R-squared	0.41	0.41		0.41	0.41	0.41	0.41

Absolute value of t statistics in parentheses
* significant at 5%; ** significant at 1%

Table 4: Regression Results: Myanmar

All variables in logs except the dummy variable for protected status

Dependent variable: Log odds ratio, cumulative forest cleared %, 2014

	Random Sample (10,000 obs.)			20% Random Sample		All Observations	
	IV	Bootstrap IV	Spatial IV	IV	Bootstrap IV	IV	Bootstrap IV
	(1)	(2)	(3)	(4)	(5)	(6)	(7)
Distance from road	-0.188	-0.188	-0.186	-0.181	-0.181	-0.181	-0.181
	(21.82)**	(15.53)**	(21.67)**	(224.06)**	(26.62)**	(502.01)**	(30.26)**
Distance to nearest urban center (DU)	-0.349	-0.349	-0.340	-0.335	-0.335	-0.336	-0.336
	(17.84)**	(12.41)**	(17.50)**	(184.49)**	(26.95)**	(413.39)**	(21.88)**
DU x Primary road share	0.063	0.063	0.060	0.060	0.060	0.060	0.060
	(10.45)**	(7.29)**	(10.10)**	(105.20)**	(13.29)**	(238.00)**	(13.45)**
Slope (Std. dev. of elevation)	-0.444	-0.444	-0.440	-0.467	-0.467	-0.468	-0.468
	(14.99)**	(11.85)**	(14.97)**	(169.14)**	(20.26)**	(379.01)**	(20.54)**
Slope x Elevation	0.043	0.043	0.042	0.044	0.044	0.044	0.044
	(11.81)**	(9.23)**	(11.70)**	(131.35)**	(17.32)**	(293.71)**	(16.16)**
Protected area	-0.775	-0.775	-0.761	-0.780	-0.780	-0.782	-0.782
	(24.83)**	(20.00)**	(24.52)**	(266.24)**	(34.58)**	(596.76)**	(34.92)**
Agricultural opportunity value	0.080	0.080	0.080	0.075	0.075	0.074	0.074
	(11.50)**	(7.27)**	(11.55)**	(113.94)**	(13.67)**	(254.01)**	(14.96)**
Constant	1.335	1.335	1.431	1.319	1.319	1.324	1.324
	(12.53)**	(8.80)**	(13.27)**	(133.43)**	(19.79)**	(299.47)**	(16.68)**
Observations	10,000	10,000	10,000	1,153,615	1,153,615	5,768,082	5,768,082
R-squared	0.21	0.21		0.20	0.20	0.21	0.21

Absolute value of t statistics in parentheses
* significant at 5%; ** significant at 1%

All three countries have negative elasticities for terrain slope, as expected, and the effect of slope diminishes with elevation. Responsiveness is greatest for Bolivia and similar for Cameroon and Myanmar. Protected areas have significantly lower forest clearing in all three countries. Myanmar has the largest estimated effect, followed by Cameroon and Bolivia. As expected, forest clearing is higher in areas with higher agricultural opportunity values. The estimated response elasticity is nearly identical for Bolivia and Cameroon, and substantially lower for Myanmar.

6. Implications for Forest Clearing

The estimates reported for each country in Tables 2-4 are quite stable across estimation techniques and sample sizes, yielding very similar model-based predictions. To illustrate the implications of our results, we use the full-sample results in column (7) for a general prediction exercise: We upgrade all secondary road links to primary status, changing the primary road share to 1.0 for all observations, and predict the resulting changes in clearing for all moist tropical forest cells. Figures 7-15 display actual and predicted clearing rates for Bolivia, Cameroon and Myanmar, along with maps that highlight areas where large changes occur. Table 6 provides summary results by moist forest ecoregion; we focus on areas with maximum (80-100%) clearing.

6.1 Bolivia

Our results predict changes of significant size in four moist forest ecoregions. The greatest proportional change occurs in the Southern Andean Yungas (southern Bolivia in Figures 4, 7,8 and 9), where the area that is 80-100% cleared after upgrading is 10,390 hectares -- 6.9 times greater than the area in 2014 (1,500 hectares). The greatest absolute change occurs in the Bolivian Yungas (western part of the main moist forest area), where upgrading increases the area

of maximum (80-100%) clearing 2.8-fold, from 19,820 to 55,660 hectares. Significant change also occurs in the Southwest Amazon moist forests (central, western and northern areas), where the maximum cleared area increases from 164,790 hectares to 177,500 hectares. Figure 9 provides another perspective by identifying impacts as changes in percent cleared. Here the most striking changes are observable in the Bolivian Yungas and Southern Andean Yungas.

Table 6: Road improvement impact by moist forest ecoregion

		Area Cleared 80-100% (thousand hectares)			
Country	Moist Forest Ecoregion	2014	After Upgrading	Change	Impact Ratio
Bolivia	Southern Andean Yungas	1.50	10.39	8.90	6.9
	Bolivian Yungas	19.82	55.66	35.84	2.8
	Madeira-Tapajós moist forests	30.36	33.93	3.57	1.1
	Southwest Amazon moist forests	164.79	177.50	12.71	1.1
	Iquitos varzeá	0.15	0.16	0.01	1.1
	Monte Alegre varzeá	0.01	0.01	0.00	1.0
Cameroon	Cameroonian Highlands forests	4.17	392.00	387.83	94.0
	Northwestern Congolian lowland forests	10.19	118.02	107.83	11.6
	Cross-Sanaga-Bioko coastal forests	24.14	68.90	44.76	2.9
	Atlantic Equatorial coastal forests	11.65	24.09	12.44	2.1
	Mount Cameroon and Bioko montane forests	1.56	2.50	0.95	1.6
Myanmar	Irrawaddy freshwater swamp forests	1.04	2.98	1.95	2.9
	Irrawaddy moist deciduous forests	55.13	91.78	36.65	1.7
	Myanmar coastal rain forests	30.16	48.64	18.48	1.6
	Chin Hills-Arakan Yoma montane forests	15.28	23.92	8.63	1.6
	Northern Indochina subtropical forests	108.61	166.42	57.81	1.5
	Tenasserim-South Thailand semi-evergreen rain forests	22.43	31.51	9.08	1.4
	Mizoram-Manipur-Kachin rain forests	30.85	41.40	10.55	1.3
	Northern Triangle subtropical forests	26.08	34.81	8.73	1.3
	Kayah-Karen montane rain forests	38.97	49.90	10.94	1.3
	Lower Gangetic Plains moist deciduous forests	0.00	0.00	0.00	.

Figure 7: Bolivia - Cumulative percent cleared, 2014

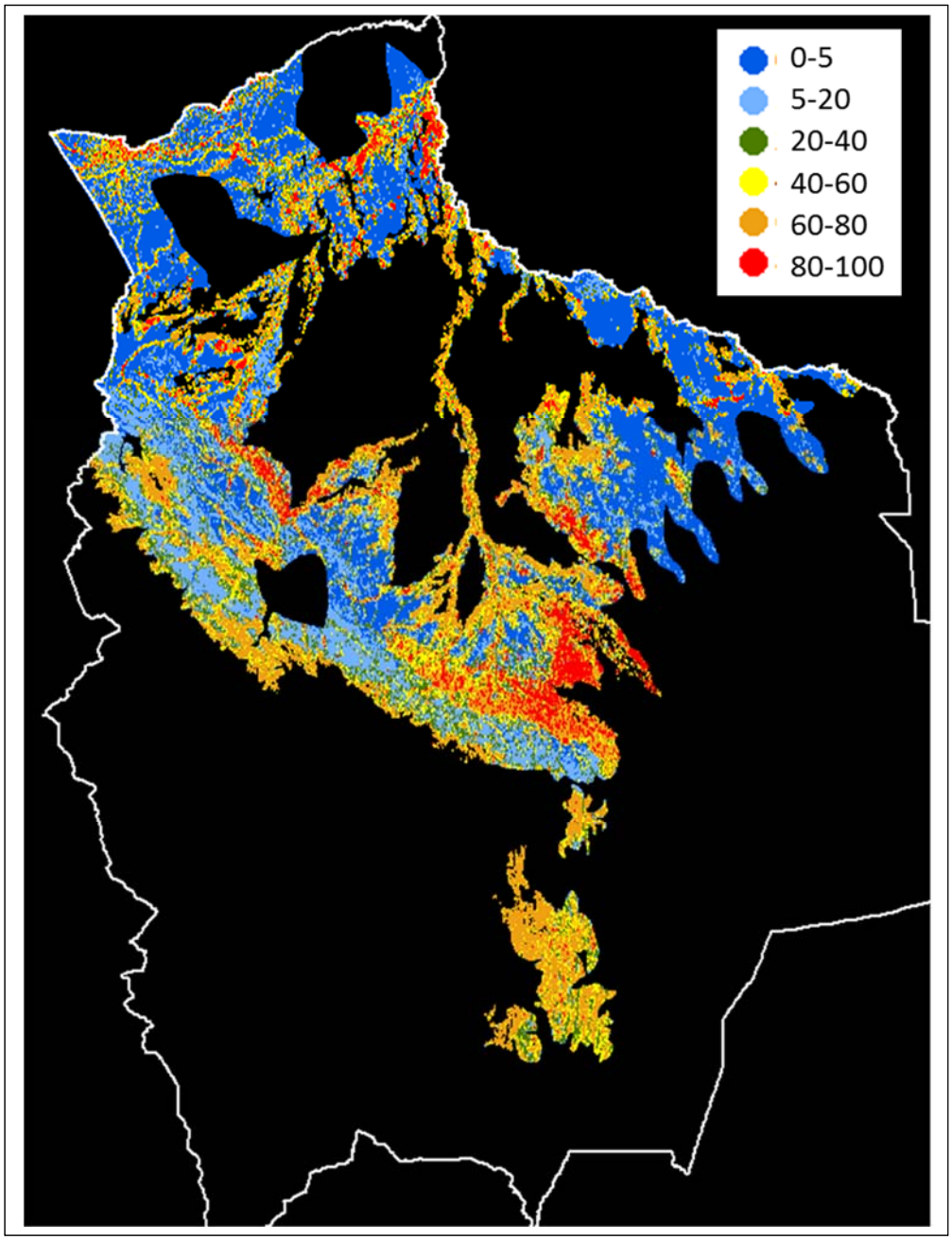

Figure 8: Bolivia - Predicted cumulative percent cleared after road upgrading

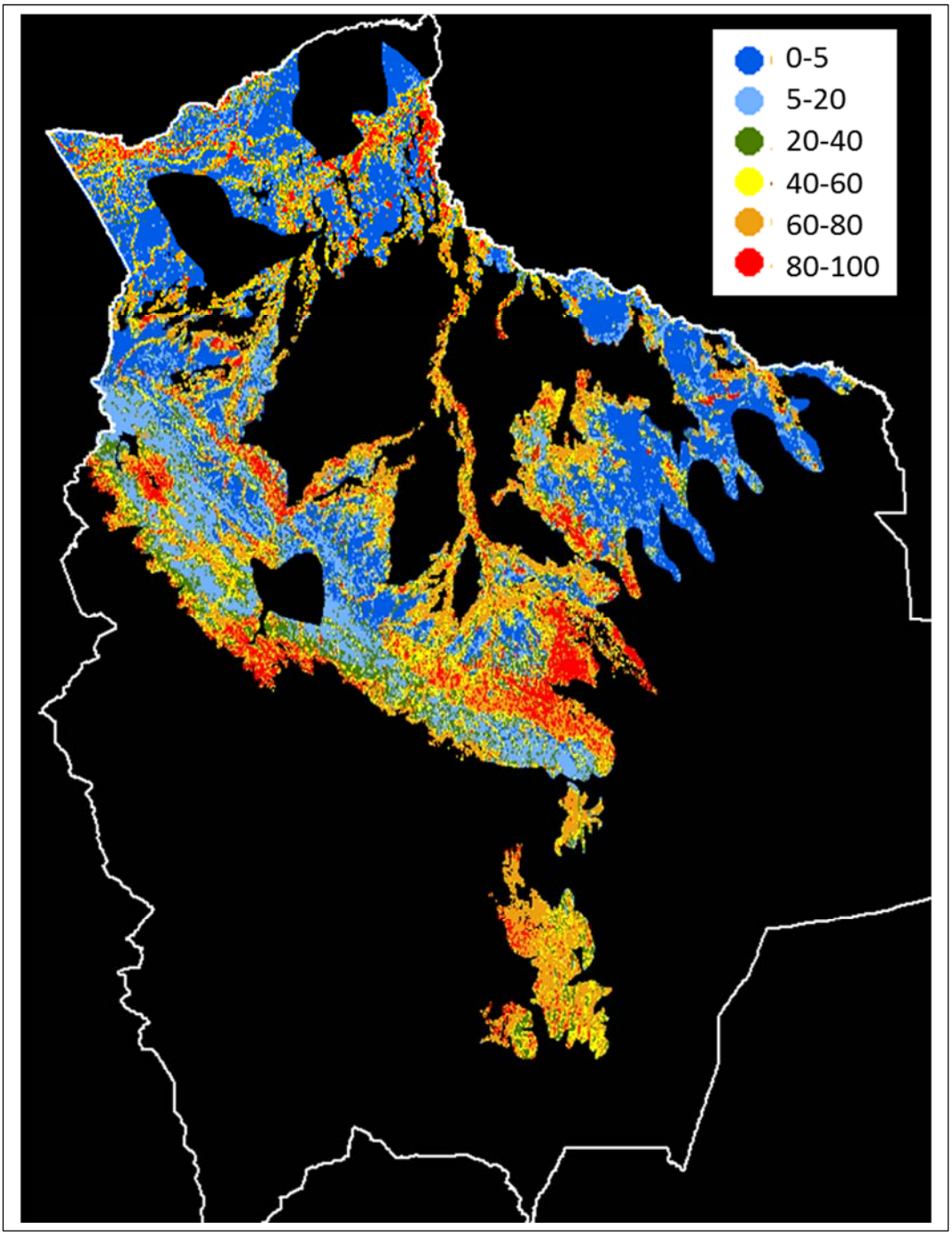

Figure 9: Bolivia - Predicted change in cumulative percent cleared

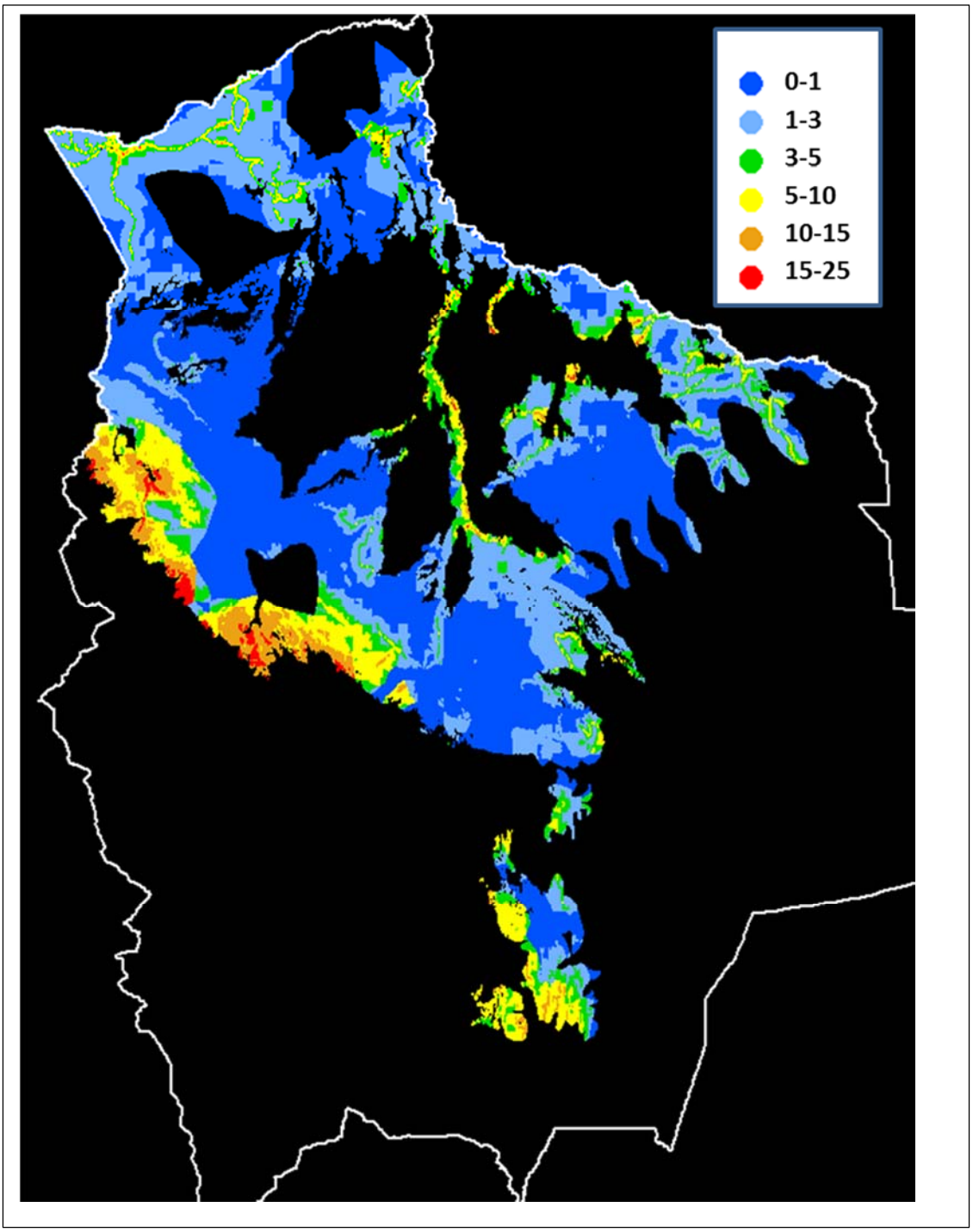

6.2 Cameroon

As Table 6 and Figures 10-12 show, Cameroon has substantially greater predicted impacts than Bolivia in both absolute and proportional terms. The greatest change by far occurs in the Cameroonian Highlands forests (extending from western to north-central Cameroon), where the 80-100% cleared area expands from 4,170 to 392,000 hectares -- a 94-fold increase. Large changes are visible in the Northwestern Congolian lowland forests (central and southeastern Cameroon), where the maximum cleared area expands from 10,190 to 118,020 hectares -- an 11.6-fold increase. Substantial expansion also occurs in the Cross-Sanaga-Bioko coastal forests (western Cameroon -- from 24,140 to 68,900 hectares) and the Atlantic Equatorial coastal forests (southwest Cameroon -- from 11,650 to 24,090 hectares).

Figure 12 provides a striking view of the pervasive changes that accompany road upgrading in Cameroon. Large areas of clearing rate change in the highest category (15-25%) are visible in southwestern, western and north-central Cameroon, along with large areas of change in the next category (10-15%) in the center, south and southwest.

Figure 10: Cameroon - Cumulative percent cleared, 2014

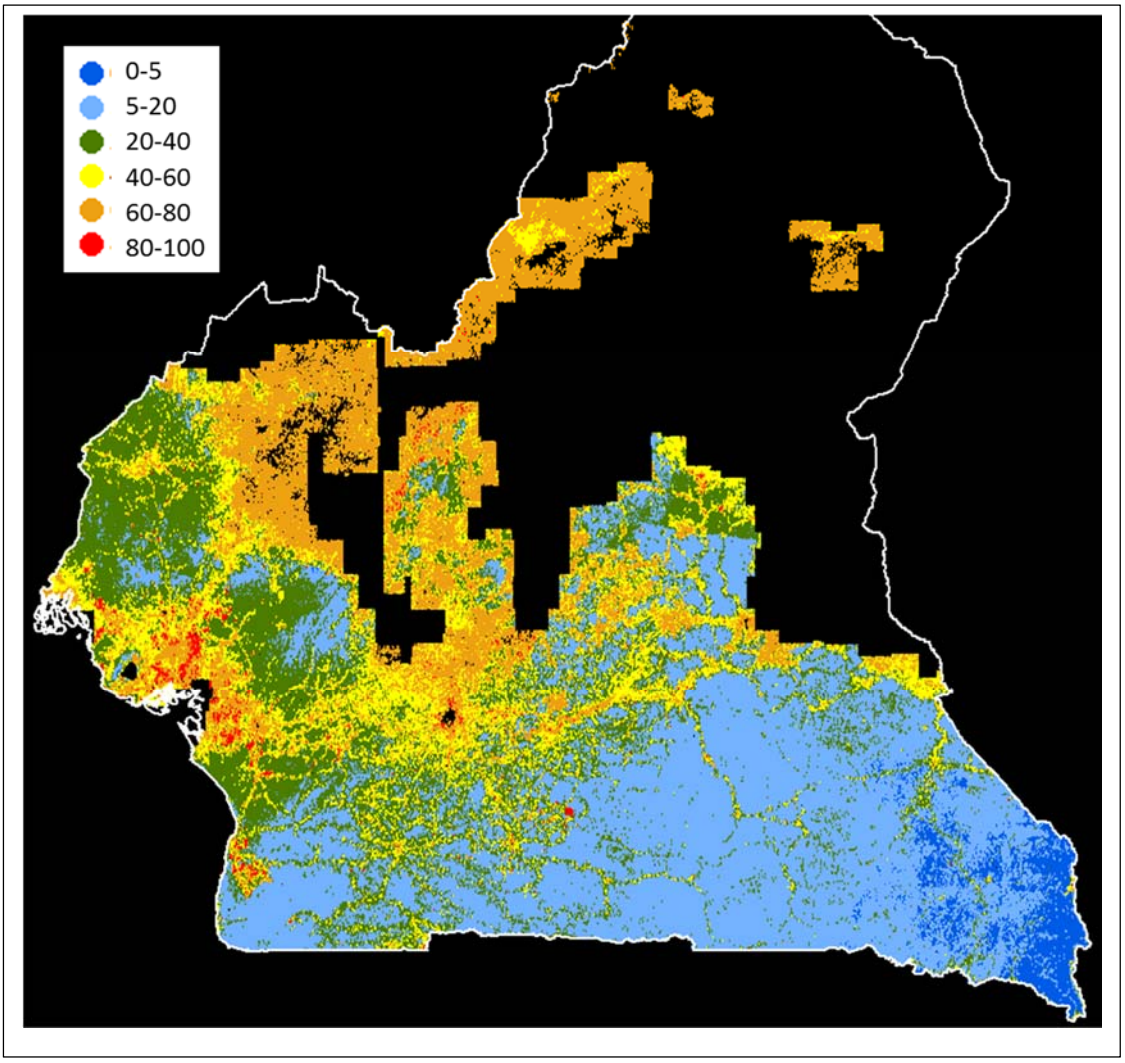

Figure 11: Cameroon - Predicted cumulative percent cleared after road upgrading

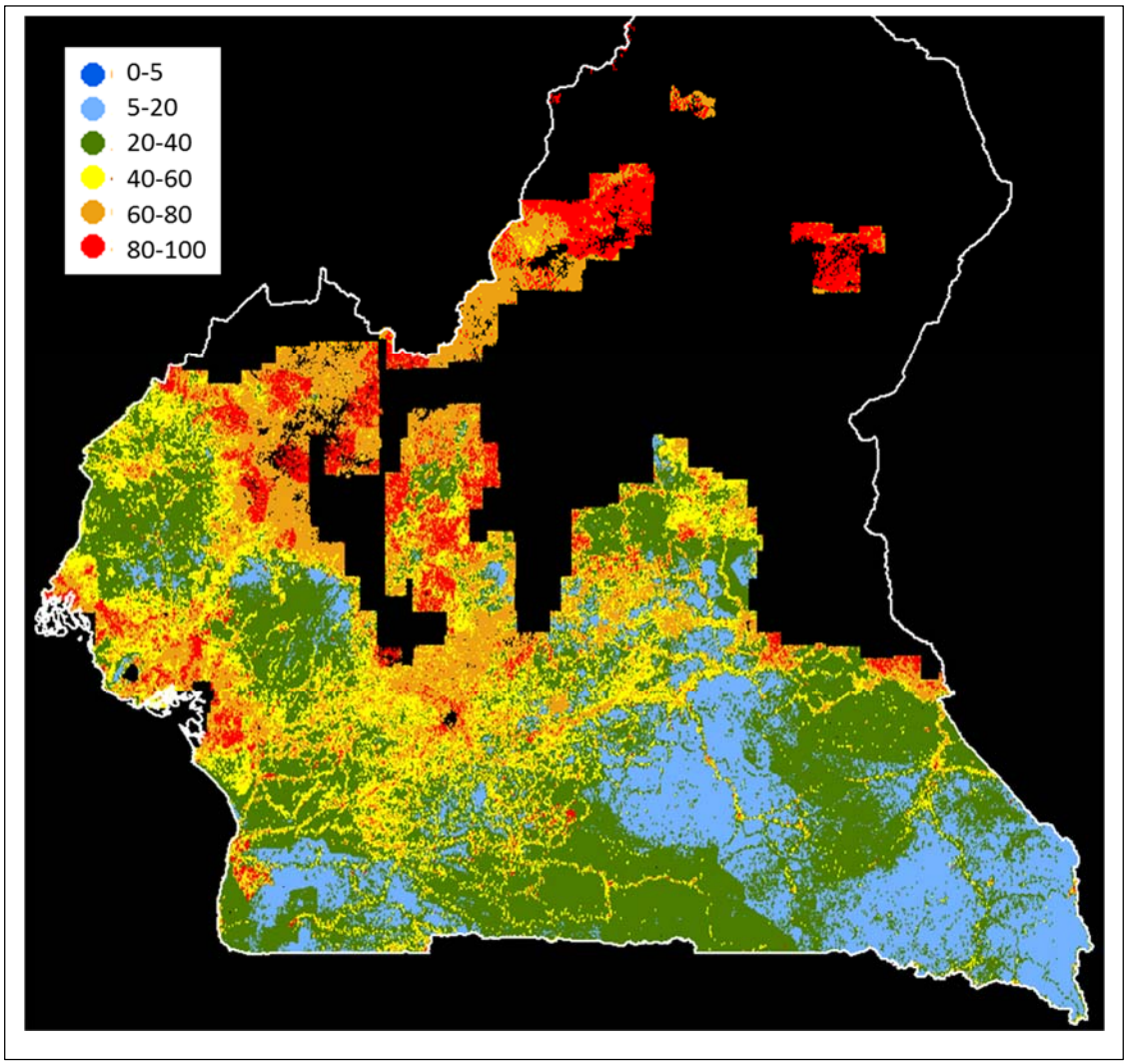

Figure 12: Cameroon - Predicted change in cumulative percent cleared

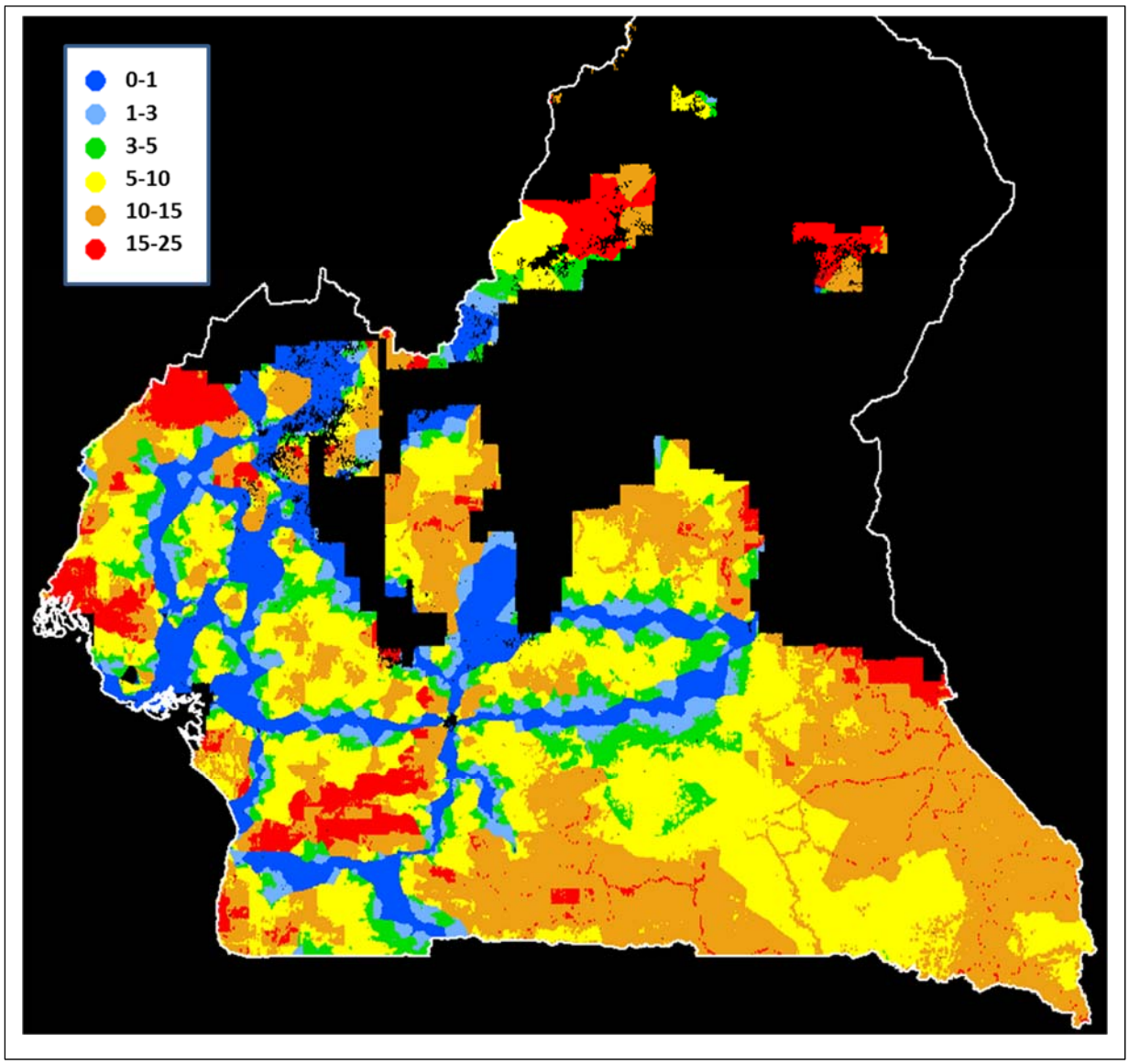

6.3 Myanmar

Table 6 and Figures 13-15 indicate that road upgrading will have widely-distributed impacts on Myanmar's moist forest ecoregions. The greatest expansion of maximum (80-100%) cleared area occurs in the Northern Indochina subtropical forests (eastern Myanmar), from 108,610 to 166,420 hectares; Irrawaddy moist deciduous forests (central Myanmar), from 55,130 to 91,780 hectares; and Myanmar coastal rain forests (western and southern Myanmar), from 30,160 to 48,640 hectares. Expansions in the range 8,000 - 11,000 hectares occur in the Chin Hills-Arakan Yoma montane forests (western Myanmar), Tenasserim-South Thailand semi-evergreen rain forests (southern Myanmar), Mizoram-Manipur-Kachin rain forests (western and northern Myanmar), Northern Triangle subtropical forests (northern Myanmar), and Kayah-Karen montane rain forests (east-central Myanmar).

Figure 13: Myanmar - Cumulative percent cleared, 2014

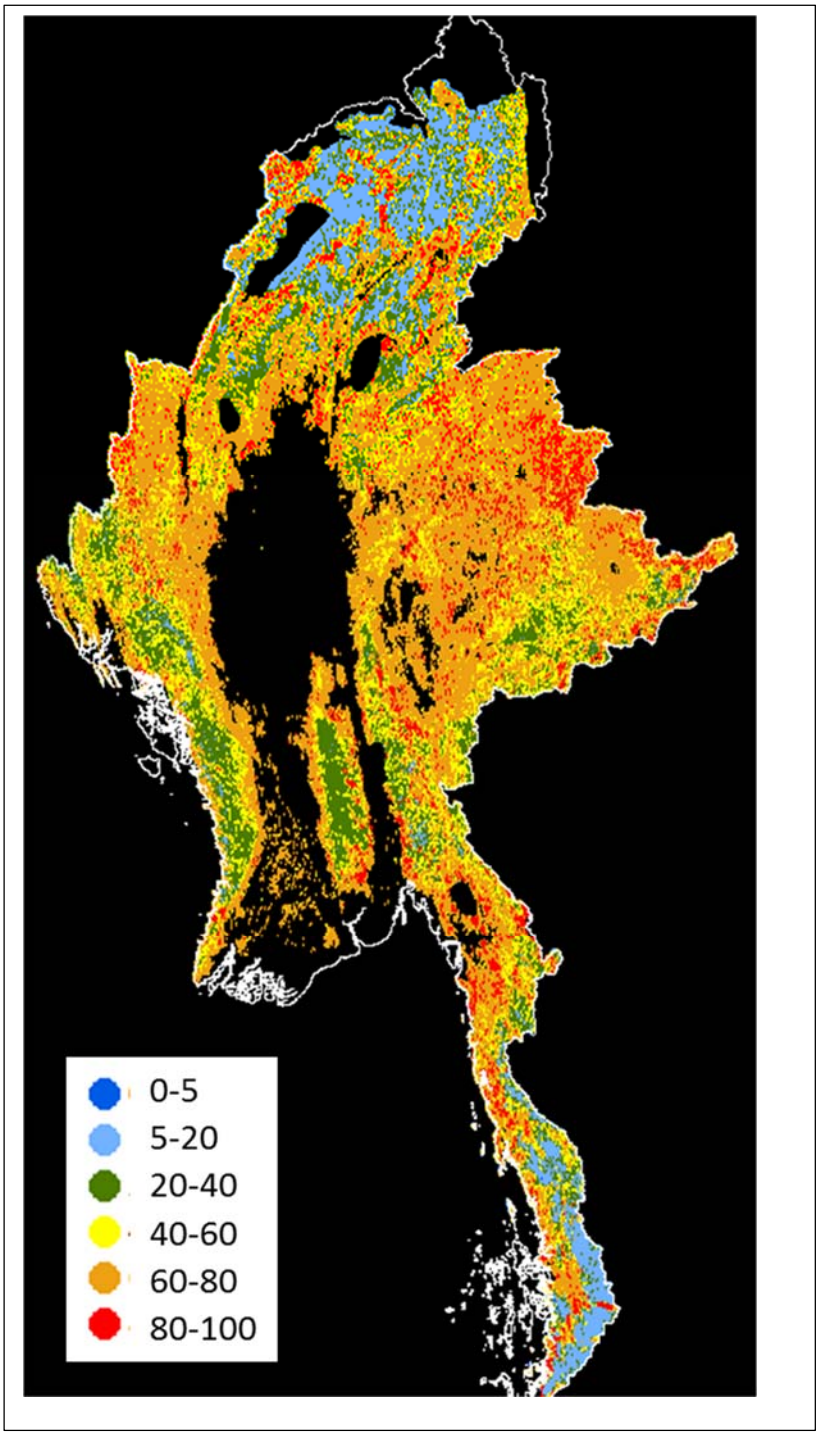

Figure 14: Myanmar - Predicted cumulative percent cleared after road upgrading

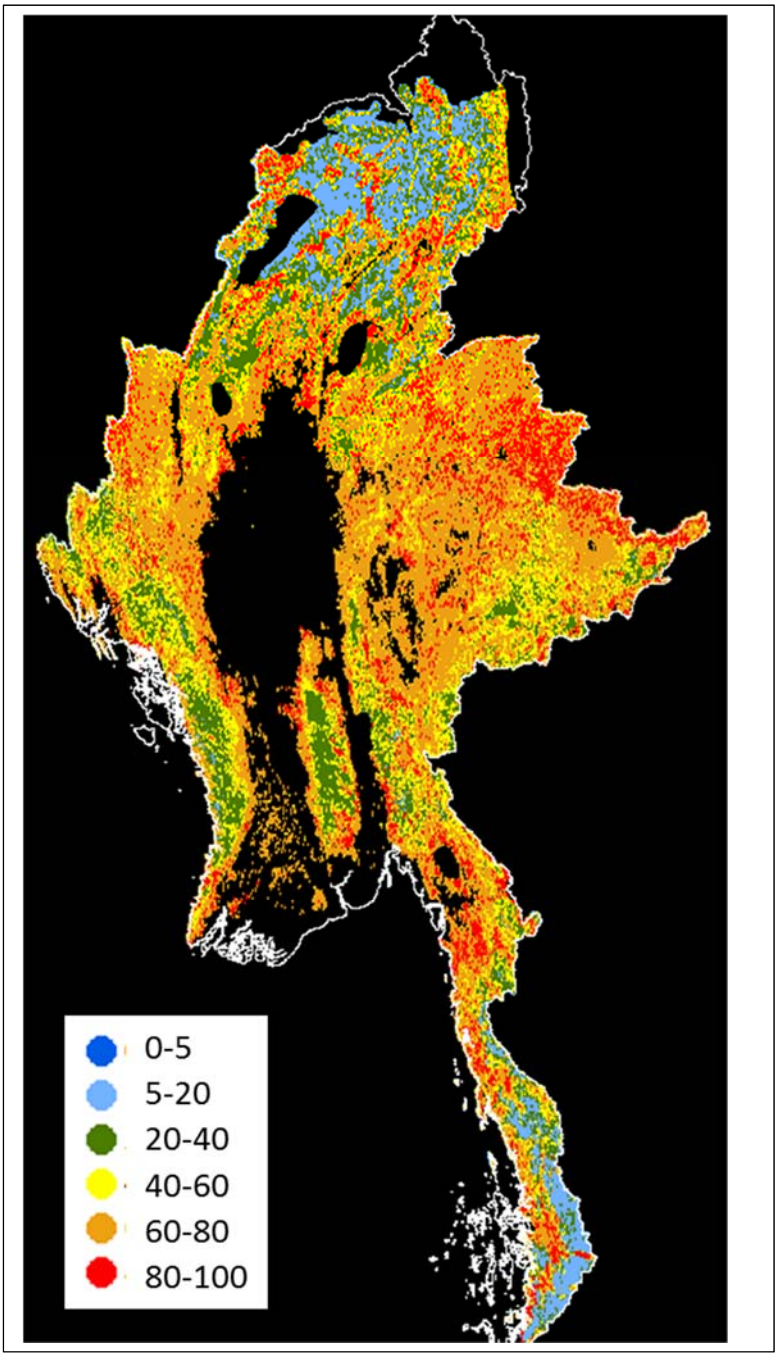

Figure 15: Myanmar - Predicted change in cumulative percent cleared

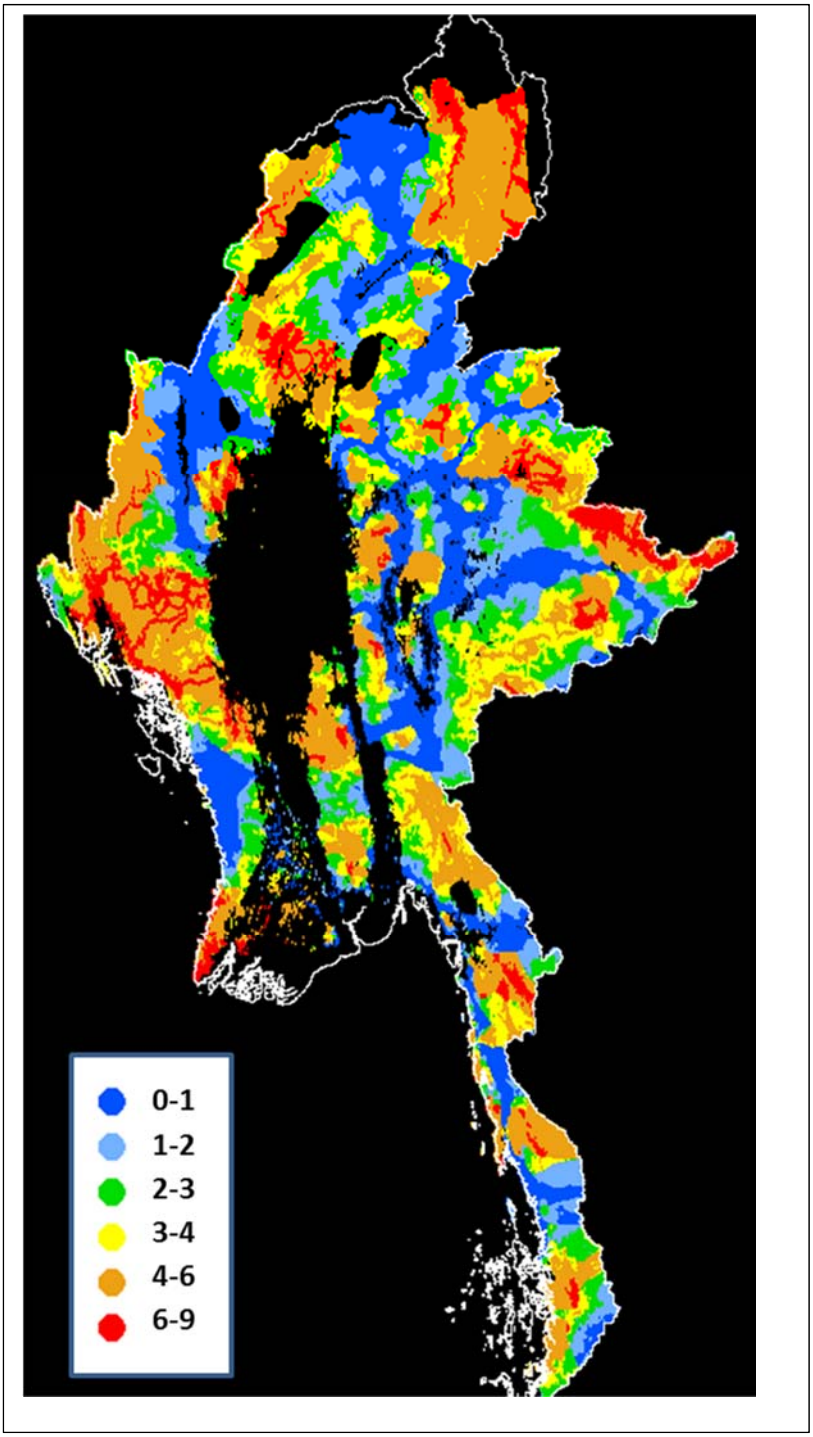

7. Incorporating Biodiversity

We develop a variety of biodiversity indicators to identify concentrations of diverse species and their vulnerability to encroachment and habitat loss in road corridors.

7.1 Species Density

We identify resident animal species in each cell using thousands of digital range maps (shapefiles) provided by the International Union for the Conservation of Nature (IUCN) and BirdLife International. We measure species density as the species count for each cell.

7.2 Species Vulnerability[8]

Species density provides critical information for assessing ecological risks, but at least three other elements are needed:

(1) ***Geographic vulnerability***, which can be proxied by ***endemicity***: the proportion of each species' range that lies within each cell. Species that reside in very few cells may be particularly vulnerable to habitat encroachment. Endemicity treats all species equally at the global level, since each species has a total count of 1. Total endemicity for each cell -- the sum of its species endemicity measures -- assigns higher values to cells inhabited by species whose ranges are relatively limited. By implication, forest clearing in higher-value cells may be particularly destructive for remaining critical habitat.

(2) **Density of endangered and critically endangered species**. Risk assessment is particularly critical for species listed as endangered by IUCN. We measure endangered species density as the count of endangered and critically endangered species in each cell.

(3) **A measure of *extinction risk*** that adds the insights of the international scientific community. We convert Red List status codes to extinction probabilities using the methodology

[8] Much of the index design work described in this section was first undertaken in a collaboration with Richard Damania for the Congo Basin countries. See Damania and Wheeler (2015).

of Mooers et al. (2008).[9] For species indicator construction, we normalize these probabilities so that a weight of 1.0 is assigned to species in the highest category (Critically Endangered). Table 7 tabulates conversions from Red List codes to normalized species weights, using four probability assignments. Three employ IUCN estimates to derive measures of extinction probability over the next 50, 100 and 500 years. The fourth draws on Isaac et al. (2007), who combine a direct extinction risk measure with a measure of each species' isolation on a phylogenetic tree.[10]

Table 7: Normalized species aggregation weights[a]

		Normalized Extinction Probabilities			
			IUCN: Future Years		
IUCN Code	Status	Isaac[b]	50	100	500
CR	Critically Endangered	1.00000	1.00000	1.00000	1.00000
EN	Endangered	0.50000	0.43299	0.66770	0.99600
VU	Vulnerable	0.25000	0.05155	0.10010	0.39000
NT	Near Threatened	0.12500	0.00412	0.01000	0.02000
LC	Least Concern	0.06250	0.00005	0.00010	0.00050
	Rounded Weight Ratios				
	CR:EN	2	2	1	1
	CR:VU	4	19	10	3
	CR:NT	8	243	100	50
	CR:LC	16	20,000	10,000	2,000

[a] Data source: Mooers et al. (2008).
[b] From calculations by Mooers et al., based on Isaac et al. (2007).

Table 7 shows that Isaac's inclusion of the phylogenetic isolation factor changes the weight ratios substantially, particularly for species in the lowest threat category (Least Concern). We explore the implications for hypothetical areas A and B in Table 8. A is populated by only 2

[9] The IUCN's current classification categories are Critically Endangered, Endangered, Vulnerable, Near Threatened and Least Concern.
[10] A phylogenetic tree is a branching tree diagram that traces the evolutionary descent of different species from a common ancestor. Species in sparse (isolated) branches of a phylogenetic tree are relatively unique, since they share common descent patterns with fewer other species.

species, both rated as Critically Endangered. B is populated by 20,000 species, but all are rated as of Least Concern. Our extinction risk indicator for each area is the sum of normalized extinction probabilities for resident species. Assignment of weights for Mooers' IUCN-derived 50-year extinction probabilities yields a total risk indicator of 2 for A -- twice the total for B, because each Critically Endangered species is weight-equivalent to 20,000 Least Concern species. In contrast, assignment of the Isaac weights yields an overall risk rating for B (1,250) that is 625 times greater than the rating for A (2), because each Critically Endangered Species is weight-equivalent to 16 species of Least Concern. The other two cases are intermediate, but far closer to the 50-year IUCN case.

Table 8: Implications of alternative weighting schemes

			Total Scores			
				IUCN Extinction Probabilities: Future Years		
Area	Species Count	Status (Uniform Within Areas)	Isaac	50	100	500
A	2	CR	2	2	2	2
B	20,000	LC	1,250	1	2	10

7.3 Biome Vulnerability

Measures based on animal species alone provide an incomplete accounting of biodiversity. A more complete measure would incorporate plants and insects, using indices similar to those we have developed for animals. Although no such indices exist at the requisite geographic scale, WWF has provided a first approximation by segmenting the world into 825 terrestrial ecoregions (Figure 16). WWF defines an ecoregion as “a large unit of land or water containing a geographically distinct assemblage of species, natural communities, and environmental

conditions."[11] Accordingly, we adopt the ecoregion as a general proxy for distinctive plant and inspect species, as well as animal species that are not represented in the range maps provided by IUCN and BirdLife International.

Our method for incorporating WWF ecoregions resembles our treatment of species endemicity. For this exercise, we identify all moist forest ecoregions in Bolivia, Cameroon and Myanmar (Figures 4-6). We compute the percent of total moist forest area in a country accounted for by each ecoregion. Then we compute its vulnerability index as the inverse of its area share and assign the appropriate index value to each cell. This accounting assigns high values to cells in smaller ecoregions, where clearing single cells may pose more significant threats to biome integrity.

[11] Complete information about the WWF terrestrial ecoregions is available online at http://wwf.panda.org/about_our_earth/ecoregions/.

Figure 16: WWF Terrestrial Ecoregions

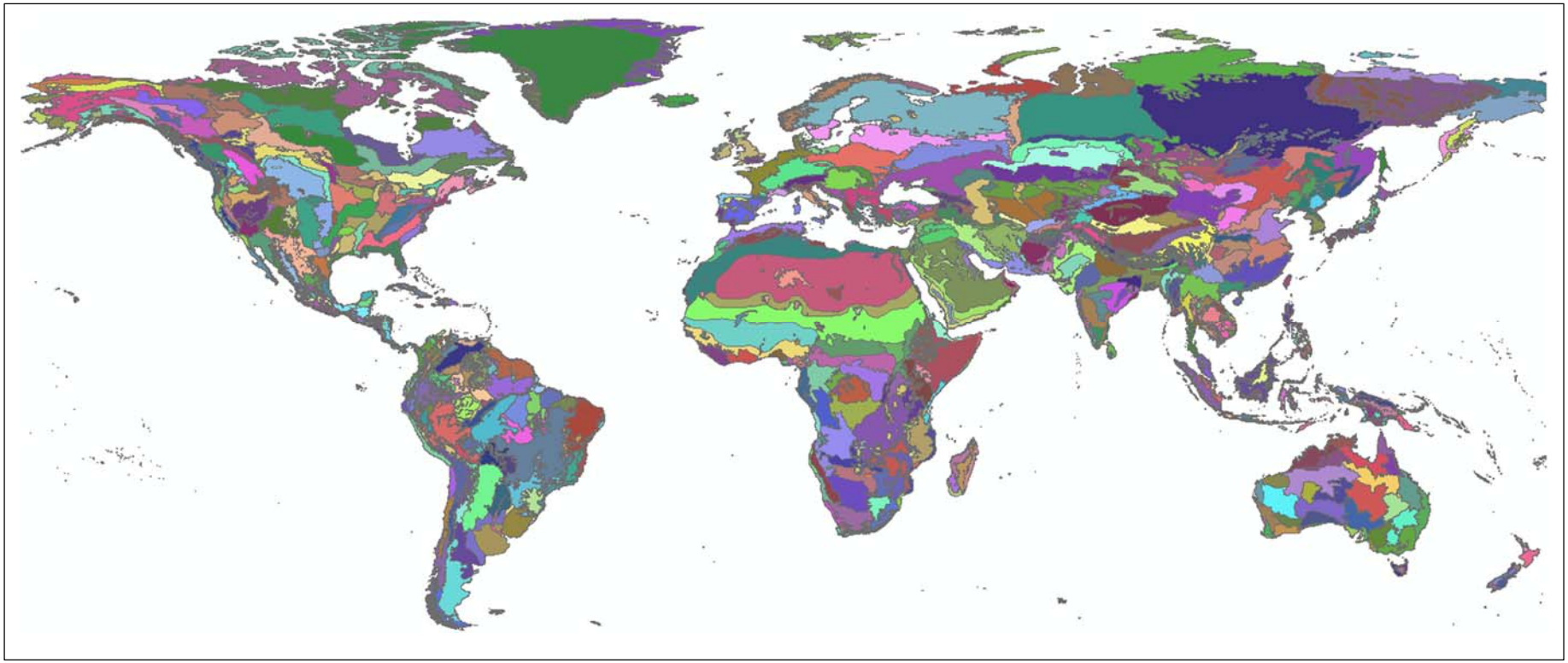

7.4 A Composite Biodiversity Indicator

The example in Table 8 suggests that alternative vulnerability indicators may yield significantly different risk metrics. For a more general assessment, we present country correlation coefficients for our seven biodiversity indicators in Table 9. These are calculated from indicator values for our 250 m cells. Two things are immediately apparent: First, pairwise correlations vary enormously: from 1.00 to -0.38 in Bolivia; 0.98 to -0.03 in Cameroon; and 0.99 to -.39 in Myanmar. Second, the same clusters appear in all three tables: correlations are high among species counts; endemicity and Isaac extinction risk; and endangered species counts and the three IUCN extinction risk indicators. The biome indicator is a distinct outlier in all three tables, with pairwise correlations that vary from positive and small to negative and relatively large.

With such potentially-huge differences in metrics, it is important for a vulnerability indicator methodology to accommodate different risk-weighting schemes in a consistent and plausible way. To accommodate diverse concerns, we adopt a conservative strategy for indicator construction. First, we divide all measures of endemicity, biome vulnerability and extinction risk by their maximum values and multiply by 100 to create indexes in the range 0-100. This ensures comparability in measurement. Then, for each 250 m cell, we select the maximum index value as our risk indicator.

Figure 17 displays the geographic distributions of the resulting indicator. In Bolivia, peak indicator values are found in a relatively small appendage area in the east and a roughly triangular area in the northwest. High values also occur in a broad arc from the northernmost area, around to the west, and into the center-west area of the dominant moist tropical forest area. Beyond these high-value areas, the index declines progressively in gradient bands.

Table 9: Biodiversity indicator correlation coefficients - Bolivia, Cameroon, Myanmar

Bolivia

	Species Count	Endangered Species Count	Endemicity	Isaac Extinction Risk	IUCN 50-Yr. Extinction Risk	IUCN 100-Yr. Extinction Risk	IUCN 500-Yr. Extinction Risk
Endangered Species Count	0.43						
Endemicity	0.98	0.34					
Isaac Extinction Risk	0.99	0.51	0.97				
IUCN 50-Yr. Extinction Risk	0.47	0.98	0.40	0.56			
IUCN 100-Yr. Extinction Risk	0.51	0.98	0.44	0.60	1.00		
IUCN 500-Yr. Extinction Risk	0.58	0.92	0.51	0.67	0.96	0.98	
Biome (Ecoregion) Risk	-0.38	-0.16	-0.37	-0.38	-0.19	-0.20	-0.23

Cameroon

	Species Count	Endangered Species Count	Endemicity	Isaac Extinction Risk	IUCN 50-Yr. Extinction Risk	IUCN 100-Yr. Extinction Risk	IUCN 500-Yr. Extinction Risk
Endangered Species Count	0.42						
Endemicity	0.85	0.27					
Isaac Extinction Risk	0.98	0.58	0.82				
IUCN 50-Yr. Extinction Risk	0.58	0.93	0.51	0.71			
IUCN 100-Yr. Extinction Risk	0.58	0.97	0.44	0.72	0.98		
IUCN 500-Yr. Extinction Risk	0.67	0.91	0.47	0.80	0.92	0.97	
Biome (Ecoregion) Risk	0.09	-0.01	0.07	0.08	-0.03	-0.01	0.02

Myanmar

	Species Count	Endangered Species Count	Endemicity	Isaac Extinction Risk	IUCN 50-Yr. Extinction Risk	IUCN 100-Yr. Extinction Risk	IUCN 500-Yr. Extinction Risk
Endangered Species Count	0.42						
Endemicity	0.97	0.41					
Isaac Extinction Risk	0.98	0.59	0.94				
IUCN 50-Yr. Extinction Risk	0.64	0.92	0.61	0.78			
IUCN 100-Yr. Extinction Risk	0.62	0.96	0.59	0.77	0.99		
IUCN 500-Yr. Extinction Risk	0.71	0.88	0.66	0.83	0.91	0.95	
Biome (Ecoregion) Risk	-0.26	-0.26	-0.26	-0.31	-0.39	-0.34	-0.27

Figure 17: Composite biodiversity indicators: Bolivia, Cameroon, Myanmar

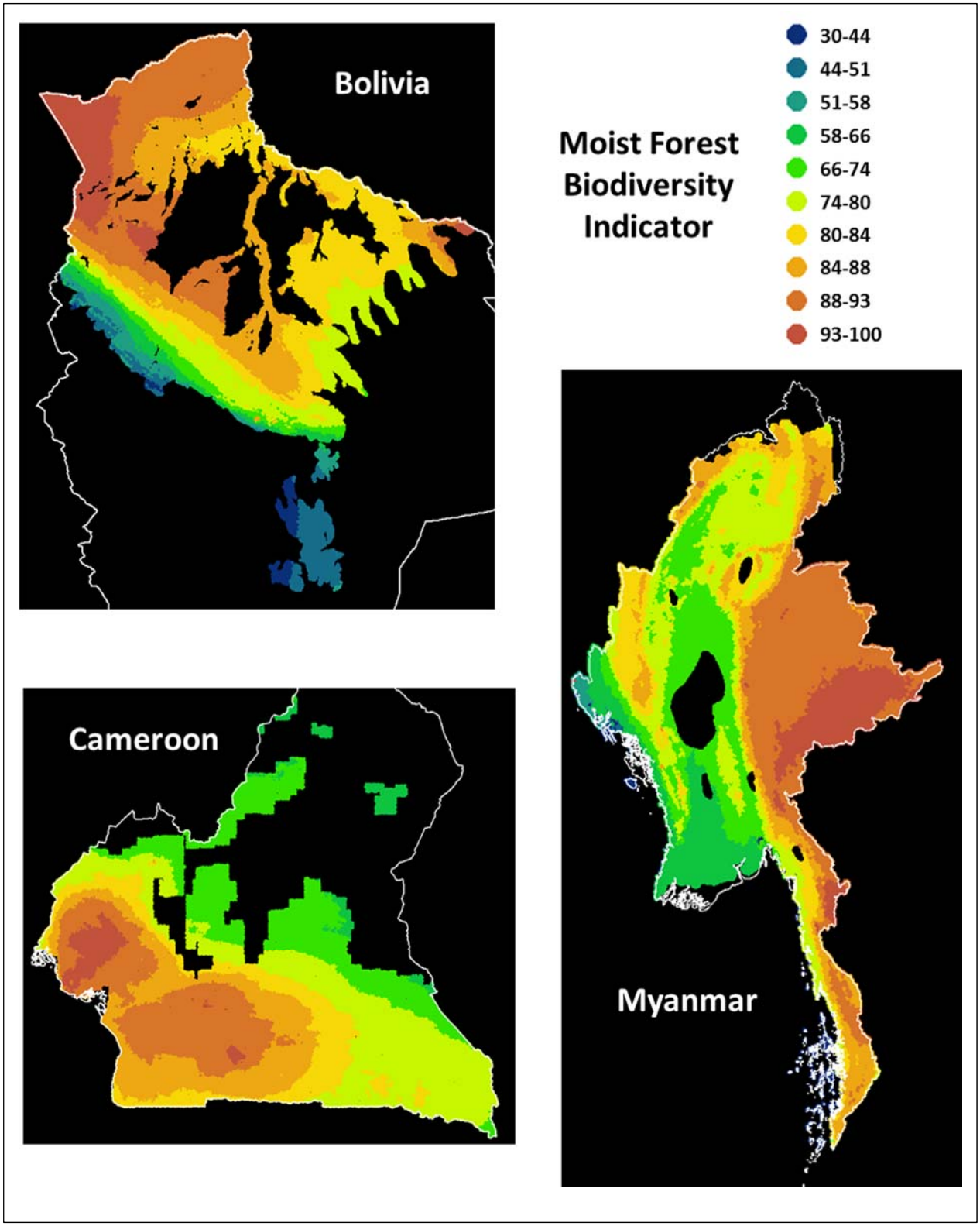

Indicator clustering is pronounced in Cameroon, with areas of peak value in the southwest surrounded by declining value gradients. In Myanmar, the highest indicator values occur in a band from center to south along the eastern border. West of these areas, values decline in gradient bands. Another band of relatively high values is visible along the country's northern and western boundaries, extending southward into west-central Myanmar.

In summary, the risk indicators displayed in Figure 17 have two clear characteristics. First, they are far from uniformly distributed: Northwest Bolivia, southwest Cameroon and eastern Myanmar account for major shares of total indicator values. Second, our construction of an "envelope" composite index from the seven subindices generates relatively smooth spatial gradient patterns that are evident in all three countries.

8. Road Upgrading and Ecological Risk

8.1 Area Calculations

We calculate expected biodiversity loss for a cell as the product of its biodiversity indicator value and the change in its cleared forest percentage induced by road upgrading. To facilitate comparison, we normalize the results to indices in the range [0 100] for each country and display the results in Figures 18-20. The Bolivian case (Figure 18) is dominated by large areas with high expected losses (index values 60 - 100) in the west and southwest, along with some road corridor areas across the north and east, along a central axis, and in the southernmost moist forest area. A striking feature of the Bolivian results is the skewed spatial distribution, including large areas where expected losses are relatively low.

The Cameroon results provide a striking contrast. As in Bolivia, some areas in the higher expected loss categories (60-100) are visible in the southwest, west and north. However, the spatial distribution of expected losses is far less skewed than Bolivia's. Cameroon's areas of

lowest expected loss generally flank the corridors of primary roads that are not candidates for upgrading. Beyond these corridors lie large areas with intermediate expected losses (40-60).

Myanmar also exhibits a more even distribution of expected losses than Bolivia's. Large areas in the highest expected loss categories (60-100) are visible in the far north, a band from the north to the east, and scattered areas in the west and south. Flanking these areas are large areas with intermediate expected losses (40-60). Again, areas with the lowest expected losses are in corridors flanking roads that already have primary status.

Figure 18: Bolivia - Index of expected biodiversity loss from road upgrading

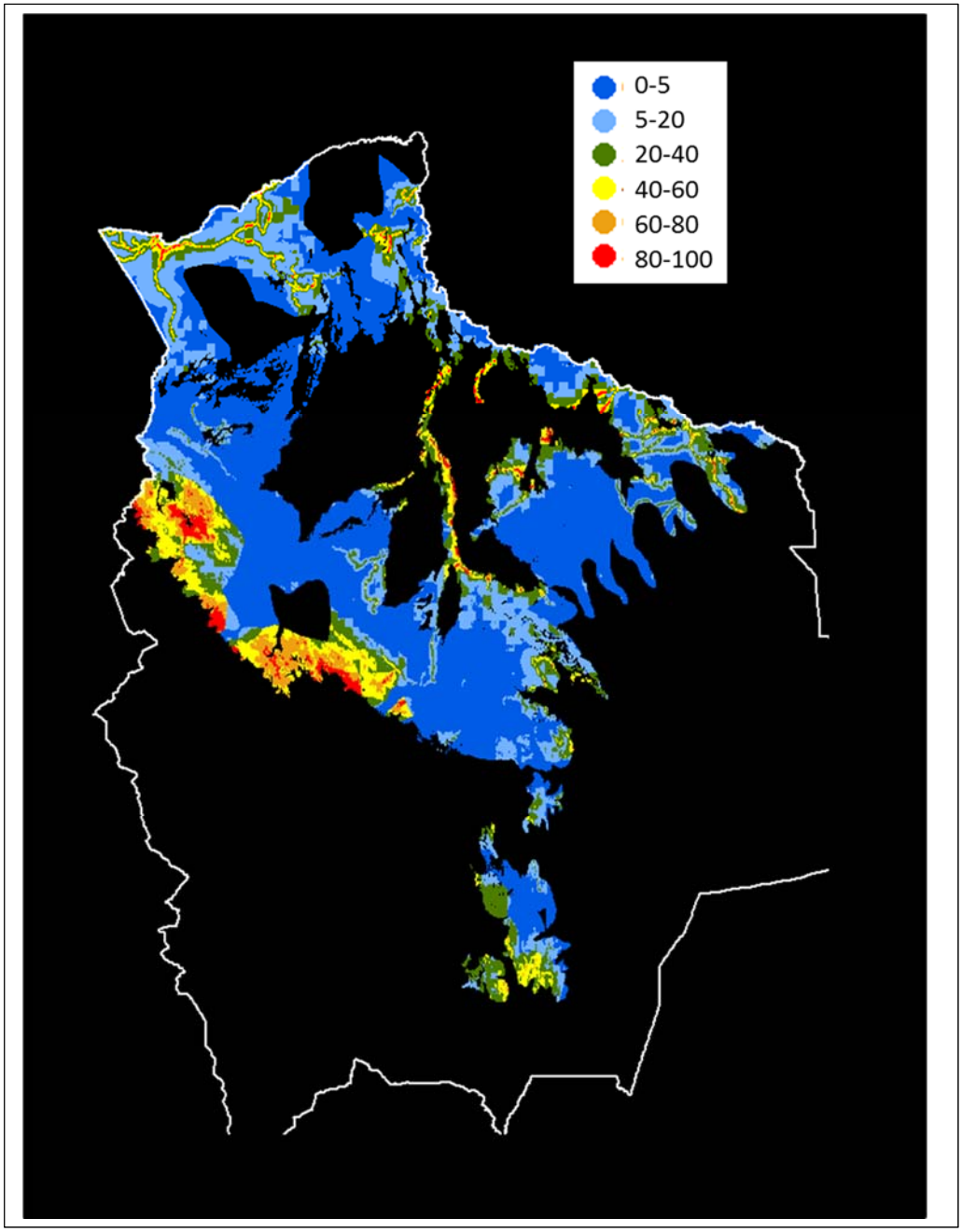

Figure 19: Cameroon - Index of expected biodiversity loss from road upgrading

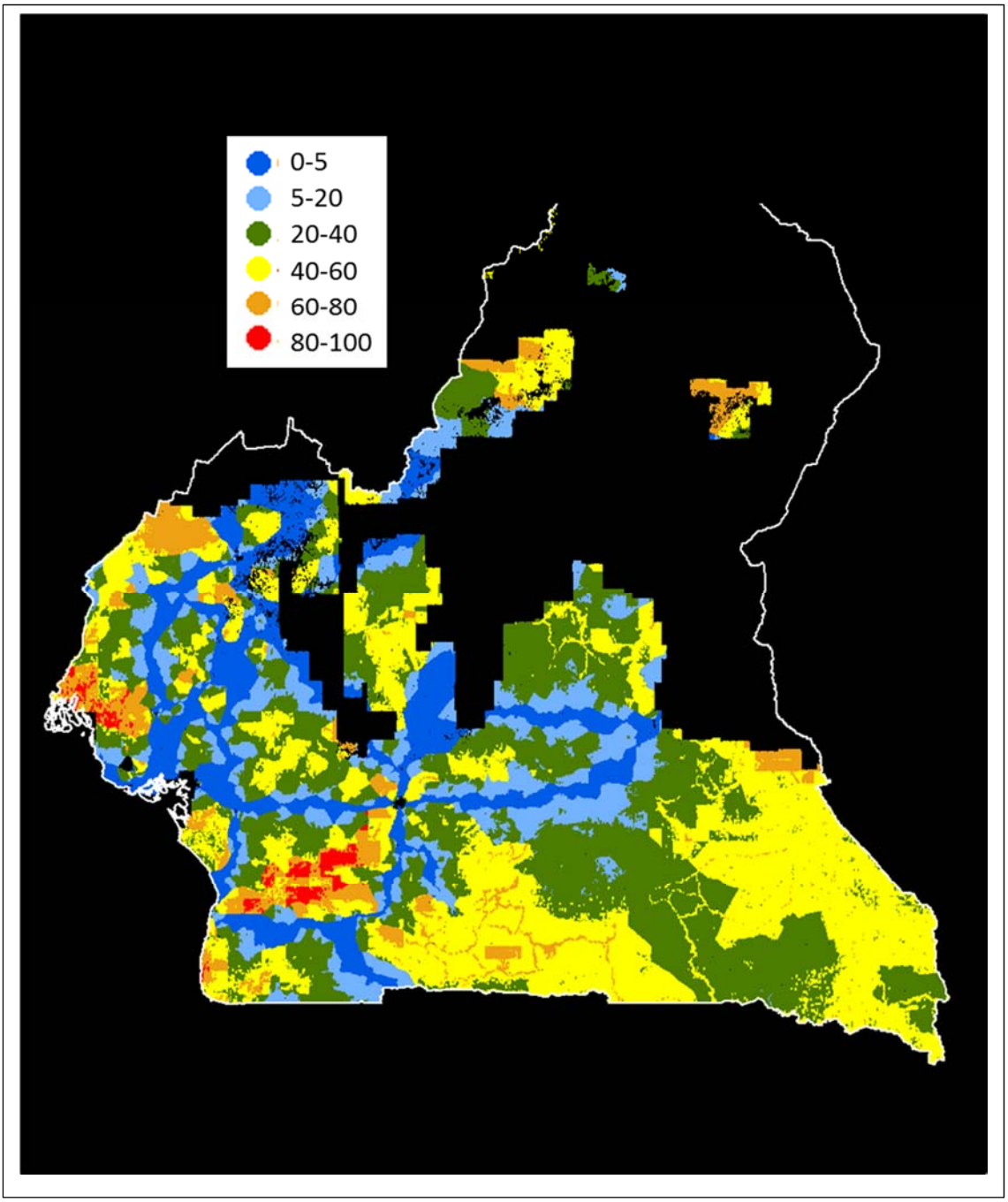

Figure 20: Myanmar - Index of expected biodiversity loss from road upgrading

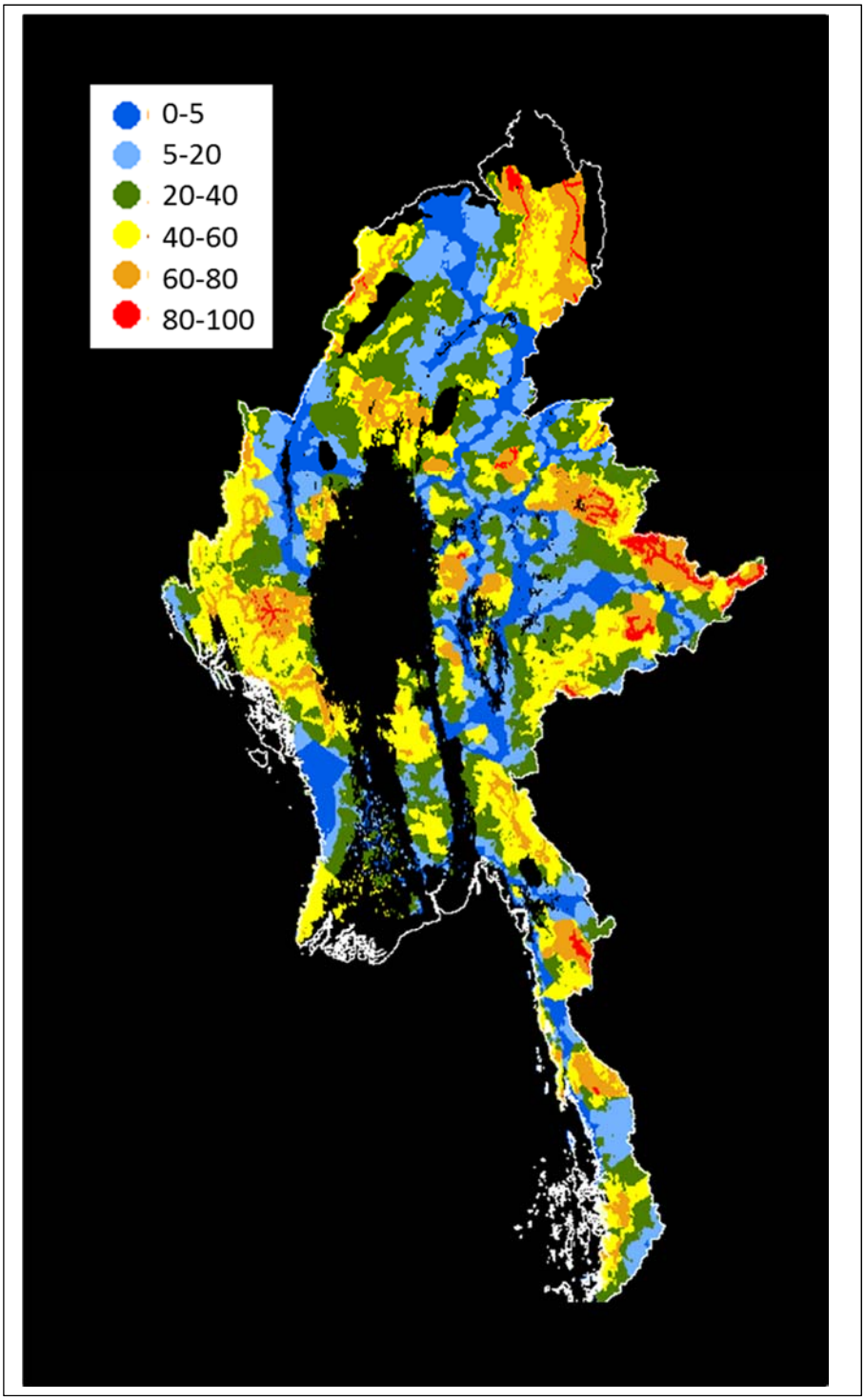

8.2 Identifying Critical Road Links

Since our methodology ties forest clearing impacts to specific road links, we can also use our high-resolution database to grade those links by expected biodiversity losses when upgrading occurs. We compute mean expected losses in corridors extending 10 km on either side of the Delorme-identified secondary road links in moist forest areas. We normalize to the range [0-100] for ease of comparison. Figures 21-23 identify the road corridors where a generalized road upgrading program is expected to produce the greatest losses in biodiversity value.[12] The maps highlight the highest four deciles (purple (90-100); red (80-90); orange (70-80); yellow (60-70)), along with primary road links where upgrading does not occur (blue).[13]

In Bolivia (Figure 21), the largest clusters of critical road links are in the center-north and far south, with smaller clusters visible in the north, east and west. Their relatively skewed spatial distribution reflects Bolivia's skewed area distribution of expected losses (Figure 18). In contrast, the distribution of critical corridors in Cameroon (Figure 22) reflects its more evenly-distributed expected losses from road upgrading (Figure 22). Road clusters in the most critical (purple) category are visible in the southwest, west and north, frequently alongside red clusters. Critical links in the lower priority (orange and yellow) categories are more widely scattered. Like Cameroon, Myanmar (Figure 23) exhibits a more even distribution of critical road corridor clusters than Bolivia. Large clusters of the most critical (purple) corridors are visible in the east, with smaller clusters linked to next-priority (red) corridors in the north, west and south. Again, clusters in the lower priority categories (orange and yellow) are widely scattered.

---

[12] This exercise focuses on the impact of generalized secondary road upgrading. It incorporates a network analysis methodology that can also be used to estimate expected losses associated with upgrades from secondary to primary status in individual road corridors. This would entail identifying all road segments linked to the closest urban market via these corridors, calculating the change in distance shares for the relevant secondary and primary road links, and predicting the forest clearing impact in all cells lying closest to the affected road links.

[13] Many Delorme road links are short; long colored road lengths in Figures 21-23 incorporate successive short links.

To summarize, the illustrative applications in this section provide high-resolution spatial measures that can inform environmentally-sensitive road upgrading programs. We use our econometric results and composite ecological vulnerability indicators to measure expected biodiversity losses for moist tropical forest cells, each of which is linked to the nearest urban market by roads at varying quality levels. Our approach identifies areas where road upgrading will produce high expected biodiversity losses, as well as road corridors that are particularly vulnerable. Since road improvement will inevitably accompany rural development, we believe that identification of ecologically-vulnerable areas and road corridors can make two useful contributions to infrastructure planning. First, with limited budgets, it can help steer road upgrading programs toward corridors where expected biodiversity losses are minimized. Second, it can highlight vulnerable areas where additional conservation measures may be warranted.

Figure 21: Bolivia - Ecologically high-risk road corridors

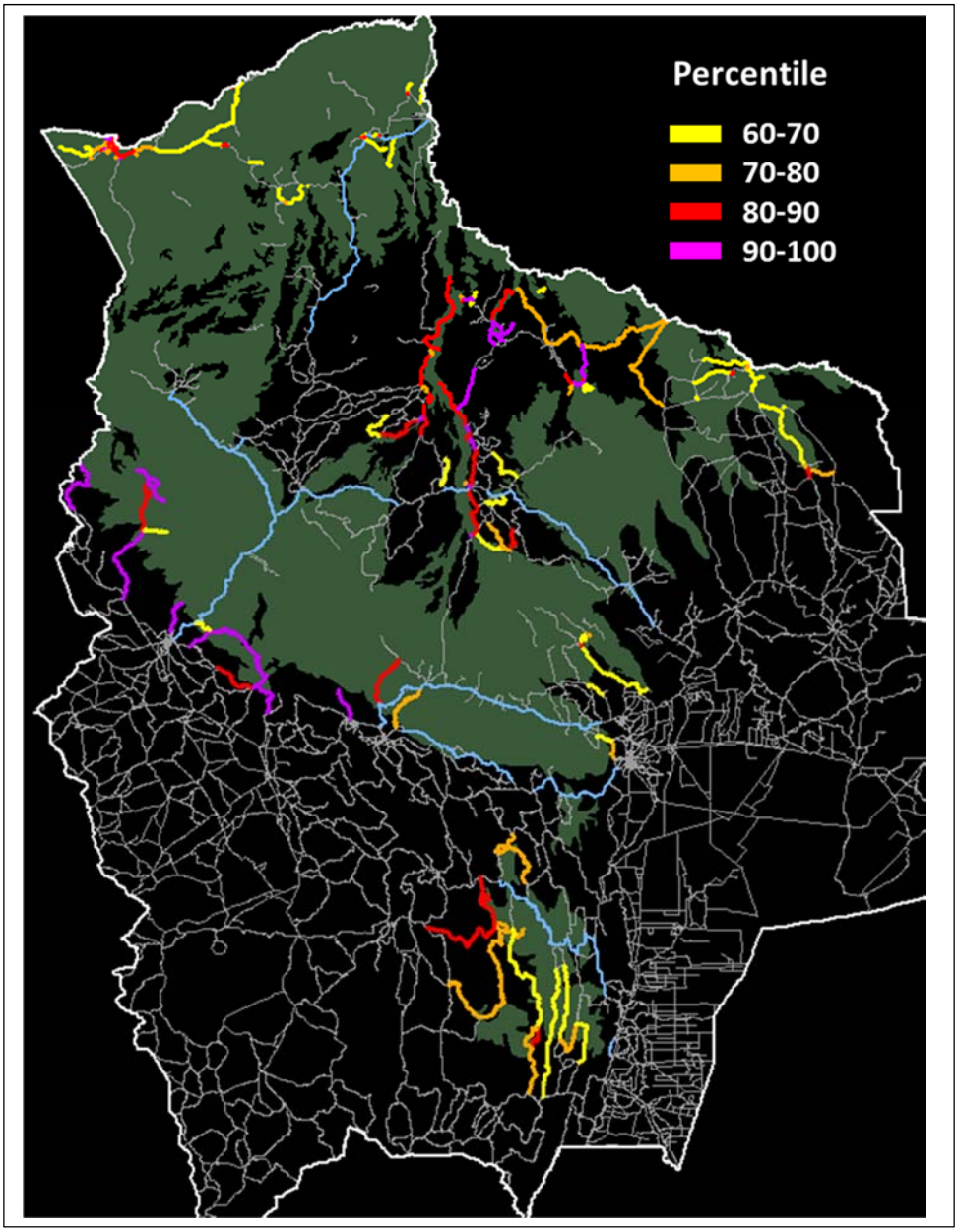

Figure 22: Cameroon - Ecologically high-risk road corridors

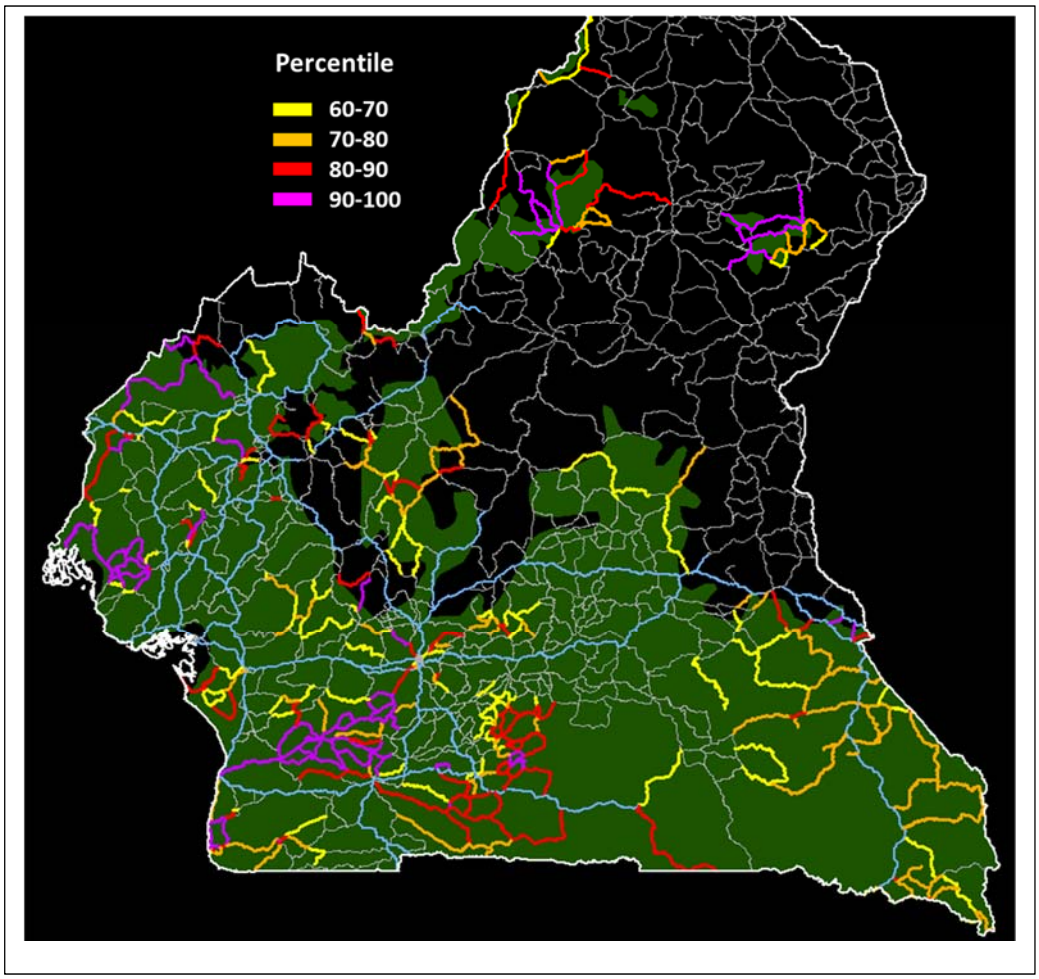

Figure 23: Myanmar - Ecologically high-risk road corridors

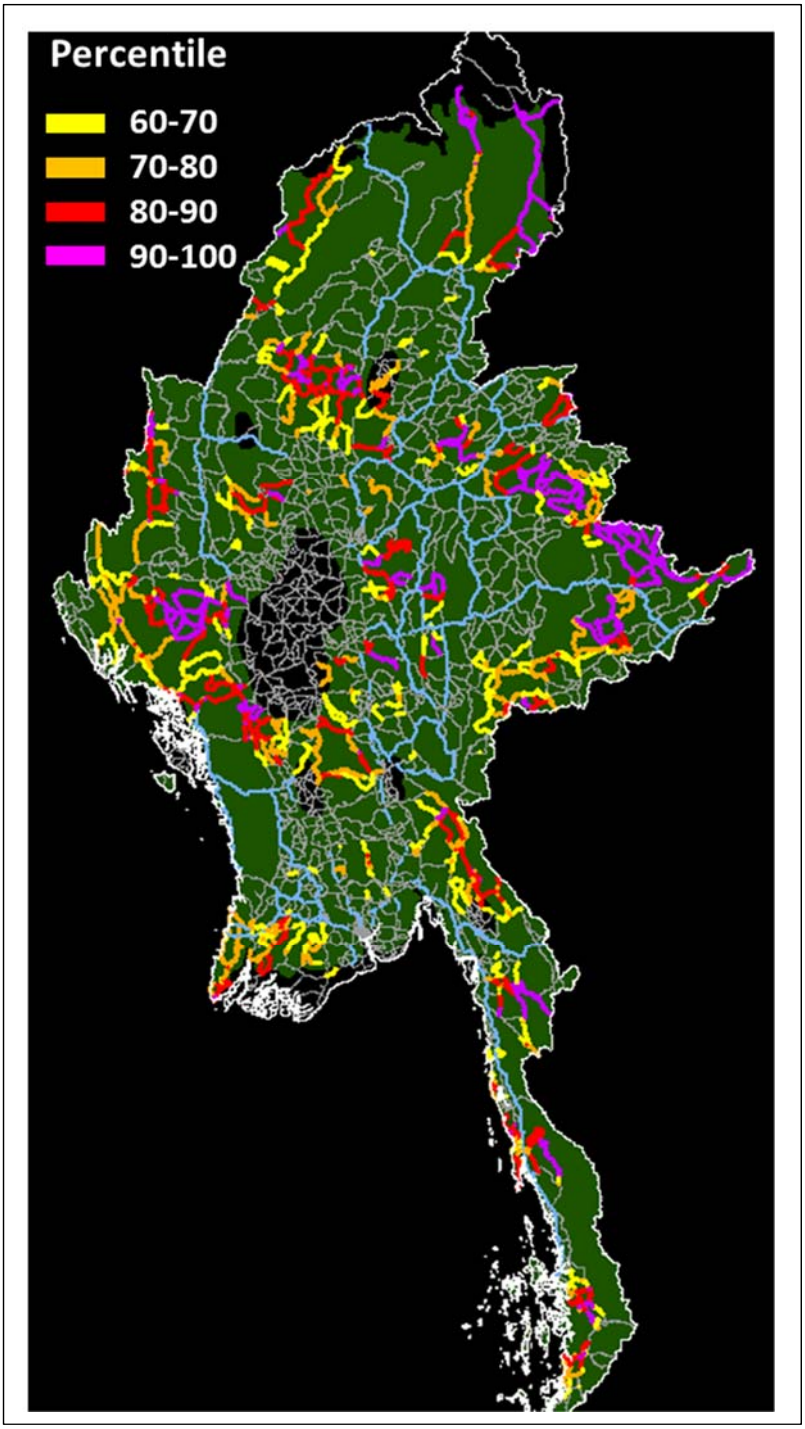

9. Summary and Conclusions

In this paper, we have developed, estimated and applied a spatially-explicit model that links road upgrading to forest clearing and biodiversity losses in moist tropical forest areas. We have chosen one World Bank IDA country from each major tropical forest region (Latin America (Bolivia), Africa (Cameroon), and Asia (Myanmar)) for illustrative purposes. However, our approach is applicable to every moist tropical forest country because we employ standard global databases:[14] High resolution forest-clearing information from Hansen et al. (2013); information on biodiversity and protected areas from IUCN and WWF International; digital road maps from Delorme, Inc.; digital elevation maps from DIVA-GIS; and information on agricultural opportunity values from Deveny et al. (2009). Using the 30 m Hansen data, we estimate forest clearing rates for all 250 m cells in the moist tropical forests of Bolivia, Cameroon and Myanmar. For each 250 m cell, we use GIS to measure the distance to the closest point on the nearest road; the distance-minimizing route to the nearest urban market, with explicit measurement of distances traveled on secondary and primary roads; mean elevation; terrain slope (the standard deviation of within-cell elevation measures); the mean agricultural opportunity value of the land; and legal protection status.

We use an appropriately-specified econometric model to estimate the effects of these variables on the cumulative percent of forest cleared in 2014. We take explicit account of spatial autocorrelation, as well as simultaneity in the relationship between forest clearing and road location. Our parameter estimates for the three countries are extremely robust, with the expected signs and very high statistical significance in all cases. The estimated elasticities exhibit little

[14] The Delorme digital road maps are available for a fee; all other data sources are in the public domain.

variation across alternative samples and estimators for each country, but significant differences across countries.

We focus particularly on the variables that measure distance to the nearest market and its partition into secondary and primary road links. We find that distance response elasticities are substantially lower for primary road links, because their higher average vehicle speeds and lower maintenance costs reduce the effect of distance to market.

Econometric measurement of road quality effects enables us to estimate the deforestation impact of programs that upgrade secondary roads to primary status. To illustrate our methodology, we explore the impact of upgrading all secondary roads to primary status in the moist tropical forest regions of Bolivia, Cameroon and Myanmar. We find highly non-uniform spatial distributions, with significant impacts in some areas of all three countries, and effects that are more evenly distributed in Cameroon and Myanmar than in Bolivia.

With our model-based predictions in hand, we measure biodiversity risk in each 250 m cell using ecoregion information from WWF International and thousands of species range maps from IUCN and Birdlife International. We develop seven measures that incorporate biome status, species density, endemicity, and extinction risk. We find weak bivariate correlations for some of these measures, so we develop a composite index for each 250 m cell by selecting the highest of the seven, each normalized to the range [0 100].

We compute an expected loss measure for each cell by multiplying its composite biodiversity index by the predicted increase in forest clearing percent from secondary road upgrading. We map the results to identify priority areas with high expected losses, along with ecologically-critical road corridors within those areas. We find highly diverse patterns of

expected forest clearing and biodiversity loss that would be difficult to anticipate without this kind of analysis.

In summary, our methodology combines high-resolution spatial databases and appropriate econometric estimation to produce measures of expected forest clearing and biodiversity loss from secondary road upgrading in Bolivia, Cameroon and Myanmar. These three cases are purely illustrative, since the same supporting data are available for all tropical forest countries.

Since road upgrading will inevitably accompany rural development programs, we believe that explicit identification of ecologically-vulnerable areas and road corridors can provide two valuable types of information. First, with limited budgets, it can help steer road upgrading programs toward corridors where expected biodiversity losses will be minimized. Second, it can inform the adoption of appropriate protection measures in vulnerable road corridors and neighboring areas. Since our methodology can be applied to any country case at relatively low cost, we believe that more widespread application could provide useful assistance for environmentally-sensitive infrastructure planning.

We recognize that a full application of our approach requires investments in data assembly, geographic information systems and econometric analysis that may not be feasible for all potentially-interested parties. However, we believe that important insights can be gained by combining basic elements of our approach in a geographic analysis that roughly quantifies the agricultural potential and biodiversity value of forested areas in corridors where new road investments may occur. Such an analysis would flag potential hotspot areas with both high biodiversity value and high agricultural conversion potential.

References

Arcanda, Jean-Louis, Patrick Guillaumont, Sylviane Guillaumont Jeanneney. 2008. Deforestation and the real exchange rate. Journal of Development Economics, 86(2): 242-262.

Barbier, Edward and Joanne C. Burgess. 1996. Economic analysis of deforestation in Mexico. Environment and Development Economics, 1:203-239.

Buys, Piet, Uwe Deichmann and David Wheeler. 2010. Road Network Upgrading and Overland Trade Expansion in Sub-Saharan Africa. Journal of African Economies 19(3): 399-432. June.

Cattaneo, Andrea. 2001. Deforestation in the Brazilian Amazon: Comparing the Impacts of Macroeconomic Shocks, Land Tenure, and Technological Change. Land Economics 77(2): 219-240.

Chowdhury, Rinku Roy. 2006. Driving forces of tropical deforestation: The role of remote sensing and spatial models. Singapore Journal of Tropical Geography, 27:82–101.

Cropper, Maureen, Jyotsna Puri, and Charles Griffiths. 2001. Predicting the Location of Deforestation: The Role of Roads and Protected Areas in North Thailand. Land Economics, 77(2):172-186.

Cropper, Maureen, Charles Griffiths and Muthukumara Mani. 1999. Roads, Population Pressures, and Deforestation in Thailand, 1976-1989. Land Economics, 75(1): 58-73.

Damania, Richard and David Wheeler. 2015. Road Improvement and Deforestation in the Congo Basin Countries. World Bank Policy Research Working Paper No. 7274.

Dasgupta, Susmita, Daniel Hammer, Robin Kraft and David Wheeler. 2014. Vyaghranomics in space and time: Estimating habitat threats for Bengal, Indochinese, Malayan and Sumatran tigers. Journal of Policy Modeling (forthcoming).

Deininger, Klaus and Bart Minten. 1999. Poverty, Policies, and Deforestation: The Case of Mexico. Economic Development and Cultural Change, 47:313–344.

Deininger, Klaus and Bart Minten. 2002. Determinants of Deforestation and the Economics of Protection: An Application to Mexico. American Journal of Agricultural Economics, 84(4): 943-960.

De Pinto, Alessandro and Gerald C. Nelson. 2009. Land Use Change with Spatially Explicit Data: A Dynamic Approach. Environmental and Resource Economics, 43(2): 209-229.

Deveny, A., J. Nackoney, N. Purvis, R. Kopp, M. Gusti, G. Kindermann,, M. Macauley, E. Myers Madeira, M. Obersteiner and A. Stevenson. 2009. Forest Carbon Index: The geography of forests in climate solutions. Joint report by Resources for the Future and Climate Advisers. December

Ewers, Robert, William Laurance and Carlos Souza. 2008. Temporal fluctuations in Amazonian deforestation rates. Environmental Conservation, 35:303-310.

Hansen, M.C., P. V. Potapov, R. Moore, M. Hancher, S. A. Turubanova, A. Tyukavina, D. Thau, S. V. Stehman, S. J. Goetz, T. R. Loveland, A. Kommareddy, A. Egorov, L. Chini, C. O. Justice and J. R. G. Townshend. 2013. High-Resolution Global Maps of 21st-Century Forest Cover Change. Science 342 (6160): 850-853.

Igliori, Danilo Camargo. 2006. Deforestation, Growth and Agglomeration Effects: Evidence from Agriculture in the Brazilian Amazon. Department of Land Economy, University of Cambridge.

Isaac N., S. Turvey, B. Collen, C. Waterman and J. Baillie. 2007. Mammals on the EDGE: conservation priorities based on threat and phylogeny. PLoS One 2: e29.

Joint Research Center (JRC). 2003. European Commission Global Land Cover 2000 Project. http://bioval.jrc.ec.europa.eu/products/glc2000/glc2000.php.

Kaimowitz, D., P. Mendez, A. Puntodewo and J. Vanclay, 2002. Spatial regression analysis of deforestation in Santa Cruz, Bolivia. In C.H. Wood and R. Porro (eds) Land Use and Deforestation in the Amazon. University Press of Florida, p. 41-65.

Kindermann, G.E., M. Obersteiner, E. Rametsteiner, and I. McCallum. 2006. Predicting the Deforestation Trend under Different Carbon Prices. Carbon Balance and Management 1(15): 1–17

Laurance, William F. 2012. As Roads Spread in Rainforests,The Environmental Toll Grows. Yale Environment 360. 19 January. http://e360.yale.edu/feature/as_roads_spread_in_tropical_rain_forests_environmental_toll_grows/2485/

Laurance, William F., Miriam Goosem and Susan G.W. Laurance. 2009. Impacts of roads and linear clearings on tropical forests. Trends in Ecology & Evolution 24(12): 659-669. 11 September

Laurance, William F., Mark A. Cochrane, Scott Bergen, Philip M. Fearnside, Patricia Delamônica, Christopher Barber, Sammya D'Angelo and Tito Fernandes. 2001. The Future of the Brazilian Amazon. Science 291(5503): 438-439. 19 January.

Li, Man, Alessandro De Pinto, John M. Ulimwengu, Liangzhi You and Richard D. Robertson. 2015. Impacts of Road Expansion on Deforestation and Biological Carbon Loss in the Democratic Republic of Congo. Environmental and Resource Economics 60: 433-469

Mooers, A., D. Faith and W. Maddison. 2008. Converting Endangered Species Categories to Probabilities of Extinction for Phylogenetic Conservation Prioritization. PLoS ONE 3(11): e3700. doi:10.1371/journal.pone.0003700.

Naidoo, R., and T. Iwamura. 2007. Global-Scale Mapping of Economic Benefits from Agricultural Lands: Implications for Conservation Priorities. Biological Conservation 140: 40–49.

Nelson, Andrew and Kenneth M. Chomitz. 2009. Protected Area Effectiveness in Reducing Tropical Deforestation: A Global Analysis of the Impact of Protection Status. Evaluation Brief 7, Independent Evaluation Group, World Bank, October.

Pfaff, Alexander. 1997. What Drives Deforestation in the Brazilian Amazon? Evidence from Satellite and Socioeconomic Data. Policy Research Working Paper No. 1772, World Bank. May.

Reymondin, Louis, Karolina Argote, Andy Jarvis, Carolina Navarrete. Alejandro Coca, Denny Grossman, Alberto Villalba, Paul Suding. 2013. Road Impact Assessment Using Remote Sensing Methodology for Monitoring Land-Use Change in Latin America: Results of Five Case Studies. Inter-American Development Bank Environmental Safeguards Unit, Technical Note No. IDB - TN - 561. July.

RFF (Resources for the Future and Climate Advisors). 2011. The Geography of Forests in Climate Solutions: Price Geography. http://www.forestcarbonindex.org/maps.html

Rudel, Thomas, Laura Schneider, Maria Uriarte, B. L. Turner II, Ruth DeFries, Deborah Lawrence, Jacqueline Geoghegan, Susanna Hecht, Amy Ickowitz, Eric F. Lambin, Trevor Birkenholtz, Sandra Baptista, and Ricardo Grau. 2009. Agricultural intensification and changes in cultivated areas, 1970–2005. Proceedings of the National Academy of Science. 106 (49): 20675–20680.

San, Nu Nu, Hans Löfgren and Sherman Robinson. 2000. Structural Adjustment, Agriculture, and Deforestation in the Sumatera Regional Economy. TMD Discussion Paper No. 52, International Food Policy Research Institute, March.

Stifel, D., and B. Minten. 2008. Isolation and Agricultural Productivity. Agricultural Economics 39 (1): 1–15.

Stifel, David, Bart Minten and Bethlehem Koro. 2012. Economic Benefits and Returns to Rural Feeder Roads: Evidence from a Quasi-Experimental Setting in Ethiopia. International Food Policy Research Institute and Ethiopian Development Research Institute. ESSP II Working Paper No. 40. May

University of Maryland. 2014. Global Forest Change 2000–2012: Data Download. Department of Geographical Sciences. Available online at http://www.earthenginepartners.appspot.com/science-2013-global-forest/download.html

Vance, Colin and Jacqueline Geoghegan. 2002. Temporal and spatial modelling of tropical deforestation: a survival analysis linking satellite and household survey data. Agricultural Economics, 27(3): 317-332.

Wheeler, David, Daniel Hammer, Robin Kraft, Susmita Dasgupta, Brian Blankespoor. 2011. Economic Dynamics and Forest Clearing: A Spatial Econometric Analysis for Indonesia. Center for Global Development Working Paper No. 280. http://www.cgdev.org/content/publications/detail/1425820

Zikri, Muhammad. 2009. An Econometric Model for Deforestation in Indonesia. Working Paper in Economics and Development Studies, No. 200903. Center for Economics and Development Studies, Department of Economics, Padjadjaran University. July.